CHALMERS
UNIVERSITY OF TECHNOLOGY

# Complexity of Thyristor-based Rectifier Operation and Optimal Harmonic Mitigation Strategies

DANIEL ASPLUND
JOEL HILDESSON

DEPARTMENT OF ELECTRICAL ENGINEERING
CHALMERS UNIVERSITY OF TECHNOLOGY
Gothenburg, Sweden 2026
www.chalmers.se

BACHELOR'S THESIS 2026

# Complexity of Thyristor-based Rectifier Operation and Optimal Harmonic Mitigation Strategies

DANIEL ASPLUND
JOEL HILDESSON

Department of Electrical Engineering
CHALMERS UNIVERSITY OF TECHNOLOGY
Gothenburg, Sweden 2026

Complexity of Thyristor-based Rectifier Operation and Optimal Harmonic Mitigation Strategies
DANIEL ASPLUND
JOEL HILDESSON



Supervisor: Thorbjörn Thiringer, Company or Department
Examiner: Thorbjörn Thiringer, Department

Bachelor's Thesis 2026
Department of Electrical Engineering
Division of Power Engineering
Chalmers University of Technology
SE-412 96 Gothenburg
Telephone +46 31 772 1000

Cover: Thyristor-based Rectifier in front of medium-voltage transformer. Image source: KraftPowercon

Typeset in LaTeX
Printed by Chalmers Reproservice
Gothenburg, Sweden 2026

Complexity of Thyristor-based Rectifier Operation and Optimal Harmonic Mitigation Strategies
DANIEL ASPLUND
JOEL HILDESSON
Department of Electrical Engineering
Chalmers University of Technology

# Abstract

For high-power industrial applications that require direct current, thyristor rectifiers are widely used to convert alternate current to direct current. However, nonlinear current loads introduce harmonics into the grid. These harmonics may reduce power quality, damage equipment, and lead to difficulty complying with standards such as IEEE 519. This thesis investigates the effect that different rectifier topologies, operation, and filtering solutions have on mitigating harmonics.

This thesis sets out to evaluate harmonic mitigation strategies for various rectifier topologies in the 1-50MW load range. Using PLECS, several different passive filter types were dimensioned. Total Demand Distortion, power factor, losses and the practical complexity of these filters were then evaluated.

The results show that increasing the pulse number of the rectifiers significantly reduces the amount of harmonics that occur and the filter requirements. A 6-pulse rectifier required extensive and complex filtering to achieve acceptable results, while 12- and 24-pulse rectifiers achieved significantly lower harmonic distortion with smaller and less complex filter banks. The study indicates that overall, higher-pulse rectifier configurations with modest filtering are an adequate and practical approach to achieving IEEE 519 compliance in high-power non-linear load operations. Extensive filtering of lower-pulse systems, while capable of achieving acceptable distortion levels, may be less attractive due to the size, cost and complexity of filtering.

Keywords: harmonics, rectifier, thyristor, filtering, tdd, ieee519, filter efficiency

# Acknowledgement

Thanks to Torbjörn Thiringer at Chalmers for supervising this thesis, and Håkan Carlsson at KraftPowercon for his supervision and guidance.

Daniel Asplund, Gothenburg, May 2026
Joel Hildesson, Gothenburg, May 2026

# List of Acronyms

Below is the list of acronyms that have been used throughout this thesis listed in alphabetical order:

AHF: Active Harmonic Filter
CTPF: C-Type Passive Filter
DTPF: Dual-Tuned Passive Filter
HAF: Hybrid Active Filter
HPF: High-Pass Filter
IEEE: Institute of Electrical and Electronics Engineers
IPR: Interphase Reactor
LV: Low Voltage
MV: Medium Voltage
PCC: Point of Common Coupling
PF: Power Factor
PHF: Passive Harmonic Filter
SCC: Short Circuit Current
STPF: Single-Tuned Passive Filter
TDD: Total Demand Distortion
THD: Total Harmonic Distortion

# Contents

# 1
# Introduction

## 1.1 Background

Thyristor based rectifiers are power electronics systems that convert Alternating Current (AC) to Direct Current (DC) using thyristors. This process is called rectification. Rectification is required in several applications, including hydrogen production through electrolysis and battery charging systems [1]. However, thyristor-based rectifiers introduce significant harmonic distortion into the AC grid. These harmonic components may result in increased power losses, thermal stress and reduced equipment lifetime.

Within the rectifier system itself, harmonic currents increase conduction and losses, resulting in higher thermal stress and reduced converter efficiency and lifetime. In the upstream power grid, harmonics contribute to increased transmission losses, transformer heating, and reduced overall power quality [2]. Harmonics may also propagate to other equipment connected to the same grid where they can cause overheating in motors, malfunction of sensitive electronic equipment, interference with communication systems and contribute to resonance problems.

International standards, such as IEEE 519, dictate how much a customer connected to the grid may "pollute" the Point of Common Coupling (PCC) in the grid. In order to comply with these standards, different kinds of *harmonic filters* may be used to cancel or reduce harmonics. These filters may vary from simple circuits constructed with passive components to sophisticated power electronic systems. The complexity and cost of harmonic mitigation solutions vary significantly depending on the selected filter topology [3].

## 1.2 Purpose

The purpose of this project is to investigate and evaluate harmonic mitigation strategies for thyristor-based rectifier systems supplying high-power industrial loads. Specifically, the study focuses on achieving compliance with IEEE 519 at the point of common coupling (PCC). The work aims to compare different filtering solutions, mainly focusing on solutions based on passive components, in terms of their effectiveness in reducing harmonic distortion as well as their impact on system performance such as power factor. In addition, practical aspects such as component size, cost and complexity are considered.

To enable a consistent comparison, the systems are modeled and analyzed using simulation tools and key parameters are dimensioned based on theoretical principles. The aim of the project is to identify suitable filtering configurations for different operating conditions and to provide guidelines for selecting harmonic mitigation strategies in high-power thyristor rectifier applications.

# 2

# Theory

## 2.1 Harmonic Distortion: THD and TDD

Harmonic distortion in an AC power system can be observed as a disturbance of the ideal sinusoidal waveform. Harmonic distortion in a power system is caused by non-linear loads that draw non-sinusoidal current. These currents interact with the frequency-dependent impedance of the network, resulting in distortion. Total Harmonic Distortion (THD) and Total Demand Distortion (TDD) are key metrics used to quantify harmonic distortion in power systems. Unlike THD which can refer to both voltage and current, TDD refers only to current measurements. THD expresses the ratio of harmonic content to the fundamental component which may vary with time and changes of the load, where as TDD expresses the ratio of harmonic distortion to the maximum demand load current. Consequently, THD is less suitable for compliance assessment in industrial systems where TDD provides a more load-independent metric [4]. High THD and TDD values indicate poor power quality, which in turn can lead to equipment malfunction, overheating, and failure.

By applying a Fourier transform, a waveform can be decomposed into sinusoidal components with different frequencies and amplitudes. For a continuous-time signal x(t), the Fourier transform is given by

$$X(f) = \int_{-\infty}^{\infty} x(t)\, e^{-i2\pi f t}\, dt \tag{2.1}$$

where $(X(f))$ represents the frequency domain content of the signal.

Each component represents a pure sinusoidal component without distortion, allowing analysis of the signal in the frequency domain, see Fig. 2.1.

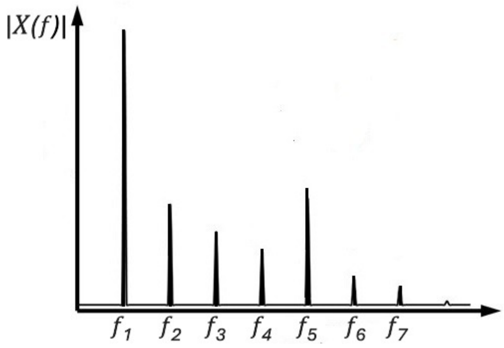


**Figure 2.1:** Example of an harmonic spectrum (FFT) illustrating magnitude (|*X(f)*|) of frequency components

$F_1$ is the fundamental frequency and $f_n = nf_1$ [5]. THD is calculated as the RMS magnitude value of all harmonic components to the RMS magnitude value of the fundamental component

$$\text{THD} = \frac{\sqrt{\sum_{n=2}^{k} h_n^2}}{h_1} \cdot 100\,\% \tag{2.2}$$

where $h_1$ is the fundamental component, $h_2 ... h_n$ are the harmonic effective values from order 2 to k, and k and n represent the last harmonics series and harmonics order. TDD is used to quantify the harmonic distortion relative to the maximum demand current of the system

$$\text{TDD} = \frac{\sqrt{\sum_{n=2}^{\infty} I_n^2}}{I_L} \cdot 100\,\% \tag{2.3}$$

where $I_L$ is the maximum demand load current. The load dependency allows TDD to enable consistent assessment of current distortion under varying load conditions, making it a more reliable metric in industrial environments [4]. TDD is widely employed in standards ensuring acceptable power quality, such as IEEE 519.

### 2.1.1 IEEE 519 - 2022

IEEE 519 (*IEEE Recommended Practices and Requirements for Harmonic Control in Electric Power Systems*) defines limits for current and voltage waveform distortion at the point of common coupling (PCC) of a power system in order to maintain acceptable power quality and ensure reliable operation [3]. The responsibility for complying with the limits defined in the standard is shared between utilities and end users connected to the PCC. IEEE 519 establishes limits for both voltage and current harmonic distortion. Voltage distortion is limited by specifying maximum allowable THD levels dependent on system voltage while current distortion limits are defined in terms of TDD. The allowable current distortion limits depend on system strength, defined by $I_{SC}/I_L$ where a higher ratio indicates a stronger system. This implies that weaker grids impose stricter constraints on connected loads making harmonic mitigation more challenging in such conditions. The requirement limits for THD and TDD according to IEEE 519 are summarized in Table 2.1 and

2.2 [3].

**Table 2.1:** IEEE 519-2022 voltage distortion limits at PCC

| V at PCC | Indiv. harmonic (%) | THD (%) |
|---|---|---|
| V $\leq$ 1.0 kV | 5.0 | 8.0 |
| 1 kV < V $\leq$ 69 kV | 3.0 | 5.0 |
| 69 kV < V $\leq$ 161 kV | 1.5 | 2.5 |
| 161 kV < V | 1.0 | 1.5 |

The levels for voltage distortion are not depending on the capacity of the operator or the customer and resulting distortion level is the combination of background distortion and load distortion created by the consumer. TDD, Table. 2.2

**Table 2.2:** IEEE 519-2022 current distortion limits at PCC for systems rated 120V - 69kV

| $I_{SC}/I_L$ | $2 \leq h < 11$ | $11 \leq h < 17$ | $17 \leq h < 23$ | $23 \leq h < 35$ | $35 \leq h \leq 50$ | TDD |
|---|---|---|---|---|---|---|
| <20 | 4.0 | 2.0 | 1.5 | 0.6 | 0.3 | 5.0 |
| 20<50 | 7.0 | 3.5 | 2.5 | 1.0 | 0.5 | 8.0 |
| 50<100 | 10.0 | 4.5 | 4.0 | 1.5 | 0.7 | 12.0 |
| 100<1000 | 12.0 | 5.5 | 5.0 | 2.0 | 1.0 | 15.0 |
| >1000 | 15.0 | 7.0 | 6.0 | 2.5 | 1.4 | 20.0 |

For even harmonics $h \leq 6$, the limits are restricted to 50% of the value obtained in the table. For current harmonics, unlike voltage harmonics, the values are not absolute but dependent on grid strength. $I_{SC}$ is maximum short-circuit current at PCC, and $I_L$ is the maximum demand load current at PCC under normal load operating conditions [4].

## 2.2 High-Power Thyristor Rectifier Configurations

Thyristor controlled rectifiers are widely used four-layer semiconductor switching devices in power electronics due to their ability to handle high voltages and currents. Since their commercial introduction in 1956, thyristor controlled rectifiers have become a well-established technology in high-power applications [6]. Due to their controllable switching characteristics, they are suitable for controlled rectifier applications, while also being low cost and simple in design. By delaying the individual enabling control signals to the thyristors, the thyristor controlled rectifier can control rectified output voltage and consequently output power [7]. The control signals are called pulses and the amount of pulses in a system is directly related to the amount of thyristors used in the rectifier configuration which are operating on phase shifted AC power. Increasing the pulse number suppresses low-order harmonics. However, this comes at the cost of increased system complexity and transformer requirements, as the transformer is the element producing phase shifted AC power sources. For an ideal $p$-pulse thyristor rectifier the dominant harmonic components in AC supply current can be expressed as [8]

$$h = pk \pm 1 \quad (k = 1, 2, 3, ...). \tag{2.4}$$

In the case of the simplest form of a three-phase thyristor rectifier, a 6-pulse rectifier, harmonics of order 5 and 7 would be primarily dominant which is particularly problematic due to their large magnitude. This makes simpler rectifier configurations impractical for high-power applications without additional harmonic filtering. Harmonic distortion caused by the thyristor rectifiers are primarily affected by pulse configuration and firing angle.

### 2.2.1 6-Pulse Thyristor Rectifier

The configuration of the simplest 6-pulse thyristor rectifier used in three-phase application can be seen in Fig. 2.2.

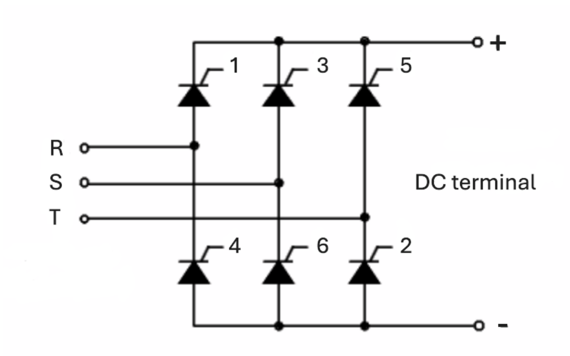


**Figure 2.2:** 6-pulse thyristor rectifier configuration with the three-phases R, S ,T and DC terminal

The thyristors are triggered using gate pulses spreat at 60° intervals in the sequence 1-6. The rectifier allows a controlled conduction sequence of the three-phases (R, S, T) to be transferred to the DC side, thereby generating a controlled pulsating DC output voltage. Control of the sequence is achieved by introducing a firing angle delay ($\alpha$) in the gate pulses which determines the instant each thyristor is activated. By varying $\alpha$, the average output voltage can be adjusted by the modified shape of the output waveform as seen in Fig. 2.3.

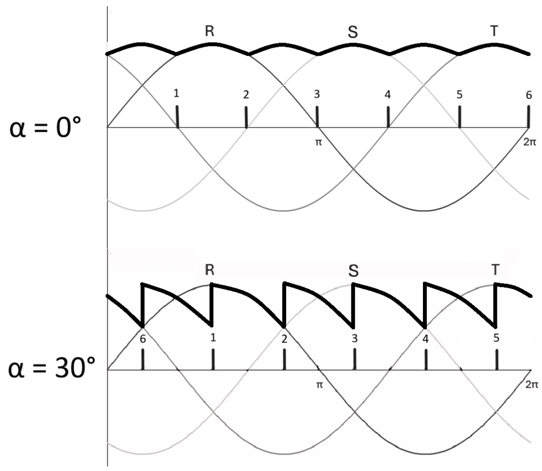


**Figure 2.3:** Three-phase Line-Line voltages and correspondent rectified output voltage (thicker line) of a 6-pulse rectifier at $\alpha = 0°$ and $\alpha = 30°$

At $\alpha = 0°$, pulse 1 is triggered 30° before $\hat{u}_R$, pulse 2 triggered 30° before $-\hat{u}_T$, resulting in maximum average DC output voltage as only the highest instantaneous voltages contributes to the rectified output. At $\alpha = 30°$, the pulses are delayed 30° and triggered as $|\hat{u}_X|$. In practical operation commutation between thyristors is rarely instantaneous due to the presence of source inductance. Instead a minor commutation interval referred to as the overlap angle occurs during which both the thyristor being turned off and the one being turned on conducts simultaneously. This overlap results in a temporary short-circuiting of the phases causing a reduction in the instantaneous output voltage and the appearance of notches in the AC-side voltage waveform. The magnitude of the overlap angle increases with higher load current and greater line inductance and reduces the average DC output voltage compared to an ideal case [9].
Output average DC voltage of an ideal case at $\alpha = 0°$ can be expressed as

$$V_{\mathrm{DC}} = \frac{1}{2\pi} \int_0^{2\pi} v_o(\theta)\, d\theta \tag{2.5}$$

Due to the repeating behavior of the rectified output voltage, every 60° segment can be integrated and multiplied, giving $V_{\mathrm{DC}} = \frac{3\sqrt{2}}{\pi} V_{LL}$ and can be approximated as $V_{DC} \approx 1.35 V_{LL}$. The firing angle dependency is described by $cos(\alpha)$ and implemented gives the complete relation

$$V_{DC} = \frac{3\sqrt{2}}{\pi} V_{LL}\ cos(\alpha) \approx 1.35 V_{LL}\ cos(\alpha) \tag{2.6}$$

At $\alpha = 90°$ the average over time output voltage is $0V$.

### 2.2.2 12–24-Pulse Thyristor Rectifiers

In three-phase uses, multi-pulse thyristor rectifiers are often realized by combining together more than one 6-pulse rectifier. By appropriately phase shifting the input phases, a smoother output is achieved. The modules consisting of 6-pulse rectifiers can either be connected in series to multiply voltage or in parallel to multiply current. The series and parallel configuration of a 12-pulse thyristor rectifier are presented in Fig. 2.4.

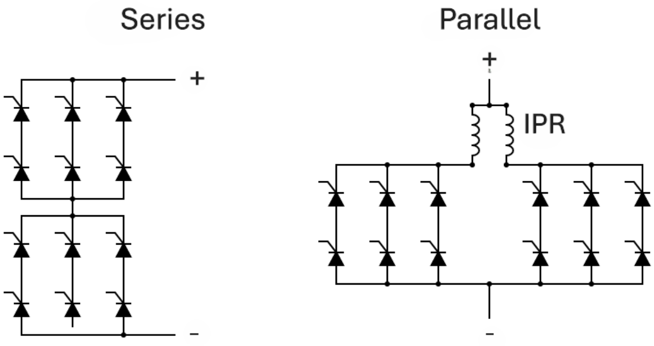


**Figure 2.4:** 12-pulse thyristor rectifier in series and parallel configuration

It is important to note that Fig. 2.4 only illustrates the basis of series and parallel connection and important elements such as the three-phase connection, phase shifting and pulse order are not included. A 12-pulse rectifier, consisting of two 6-pulse branches, each equivalent to the model illustrated in Fig. 2.2. One of the two 6-pulse branches is phase shifted 30° often using a $Y - \Delta$ winding in the transformer, causing an aligned overlap in the two branches. Voltage average of the 12-pulse parallel-connected rectifier is described equivalent to the 6-pulse voltage equation (2.6) For higher pulse configurations such as 24-pulse, the same principles used in 12-pulse series- and parallel-connection are implemented and expanded. In case of 24-pulse configurations, the four three-phase connections are shifted to be spaced equally with 15° intervals using $Z$ windings in the transformers.

An Interphase Reactor (IPR) can be used in parallel-connected thyristor rectifiers to equalize current between the branches and allow simultaneous conduction, as seen in Fig. 2.4. This improves load sharing between the 6-pulse branches, reduces ripple in output current and can contribute to a more stable operation. For the IPR to work as intended, it is important for the transformer to possess sufficiently matched leakage inductance. In a multi-pulse rectifier the IPR is governed by the basic law of inductance

$$v(t) = L\frac{di}{dt} \tag{2.7}$$

In practical dimensioning, the current is assumed to be triangular because an approximately constant voltage across the inductance causes the current to increase and decrease linearly according to

$$L_{IPR} \approx \frac{\Delta\hat{V}}{w_r \hat{I}_c} \tag{2.8}$$

where $\Delta\hat{V}$ is the peak voltage difference between connected branches, $w_r$ is based on the ripple frequency for the voltage difference, $\hat{I}_c$ is the allowed peak-value circulation current.

Transformers are essential components in multi-pulse thyristor rectifier systems. In addition to providing voltage transformation, they introduce the phase shifts between the 6-pulse branches. This enables the cancellation of characteristic harmonics and therefore reduces the harmonic distortion in higher-pulse configurations. Consequently the transformer configuration has a significant influence on harmonic distortion, commutation behavior and power factor.

The transformer leakage inductance also strongly affects the commutation process. Since the current through an inductive element cannot change instantaneously a commutation overlap angle occurs. This can in turn decrease DC output voltage and degrade PF [9]. Appropriate values of leakage inductance are therefore of interest when examining the performance and harmonic characteristics of multi-pulse rectifier systems.

## 2.3 Harmonic Filters

Harmonic filters are designed to mitigate generated harmonic distortion. They operate by providing frequency selective impedance that attenuates specific harmonic frequencies. By reducing harmonic currents and voltages, harmonic filters aim to improve power quality and by providing reactive compensation improve PF.

### 2.3.1 Passive Harmonic Filters

Passive harmonic filters (PHF) provide low-impedance paths for harmonic currents at specific frequencies and are especially effective for steady-state conditions. Their fixed design using inductors (L), capacitors (C) and resistors (R) limits adaptability to varying load conditions. The impedance ($Z$) is directly related to reactance ($X$)

$$Z = R + jX \tag{2.9}$$

where reactance represent the frequency-dependent opposition to alternating current caused by inductive and capacitive components. Unlike resistance, reactance does not dissipate energy as heat but instead temporarily stores and releases energy. Inductors store energy in magnetic field while capacitors store and release energy in electric fields, causing the current and voltage to phase shift. The reactance from inductance and capacitance

$$X_L = \omega L \qquad X_C = \frac{1}{\omega C} \tag{2.10}$$

is related as $X = X_L - X_C$. Inductive reactance increases with frequency and capacitive reactance decreases with frequency. Resonance occurs when the inductive and capacitive reactance cancel each other, resulting in minimum impedance at a specified frequency. This frequency is the tuning frequency of a filter and is the natural frequency of a LC circuit, expressed as

$$f = \frac{1}{2\pi\sqrt{LC}} \tag{2.11}$$

Important to note is that this formula often appears expressed in angular frequency ($\omega$) where $\omega = 2\pi f$. Passive filters use a quality factor ($Q_F$) to describe how closely the characteristic of the filter in practice matches that of an ideal filter described by the resonance formula (2.11). The quality factor therefore describes the filters selectivity and damping around specific frequencies. A high quality factor corresponds to a narrow bandwidth and a strong attenuation at the tuning frequency, a low quality factor results in a broader response. If it is too high, there is a risk of missing the targeted frequency while if it is too low the compensation may become insufficient. In practical applications the quality factor determines the filter bandwidth and selectivity around the tuning frequency, while additional damping is used to suppress resonances and transient overshoots. The reactive power in a three phase system is given by

$$Q = 3\frac{V_\phi^2}{X} \tag{2.12}$$

and is often used to determine the reactive capacitance in passive filter design [2][10].

#### 2.3.1.1 Single- and Double-Tuned Passive Filters

Single-tuned passive filters (STPF) provide effective attenuation of dominant harmonics, but their narrow bandwidth makes them sensitive to parameter variations which can be problematic under varying load conditions. Due to their simplicity and effectiveness, STPF are widely used for targeted harmonic mitigation in power systems. But can lead to resonance problem in a system. Typically implemented as a series CLR branch connected in shunt and tuned to a selected harmonic order, Fig. 2.5.[2][11]

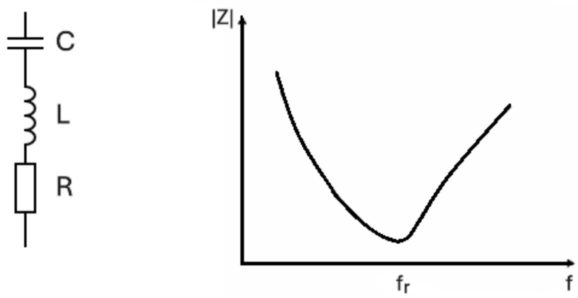


**Figure 2.5:** Configuration of a STPF and its typical characteristic impedance over frequencies with components labeled

The circuit follows the natural frequency of a LC circuit where $f_r$ is given by 2.11. In industrial applications STPF are commonly arranged as three-phase banks either in star (Y) or delta ($\Delta$) configuration depending on system grounding and insulation requirements. Delta configuration connects each phase to the other two through the filter branches forming a closed loop without a neutral point. Star connection provides each phase with an individual filter branch connected to a common point, neutral or ground, as seen in Fig. 2.5. For a STPF the quality factor is defined and directly related to the circuit parameters

$$Q_F = \frac{\omega_t L}{R} = \frac{1}{\omega_t RC} \tag{2.13}$$

where $\omega_t$ is the tuning frequency directly related to $f_r$ in Fig. 2.5. The quality factor defines the sharpness and depth of the impedance minimum at resonance. In power system applications typical quality factor ranges are in the range of $30 < Q_F < 60$ [12].

Unlike STPF, Double-tuned passive filters (DTPF) can target two harmonic frequencies simultaneously, improving compactness compared to multiple single-tuned filters. However the increased design complexity makes parameter selection more sensitive and less intuitive. Consisting of the more complex RLC network formed by combining series and parallel resonant circuits the configuration achieves two distinct resonance frequencies, Fig. 2.6.

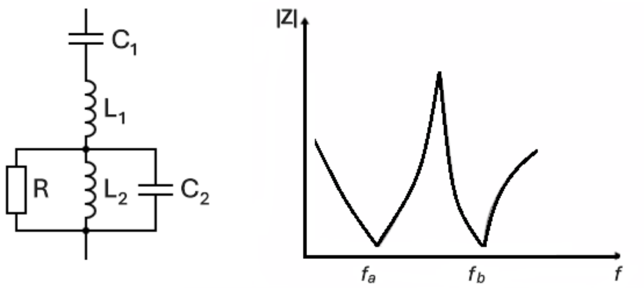


**Figure 2.6:** Configuration of a DTPF and its typical characteristic impedance over frequencies with components labeled

Similar to STPF, DTPF are usually connected in shunt and implemented in three phase banks in either Y or Δ configuration. Unlike STPF there is no direct formula to determine the quality factor and appropriate values of R are instead chosen based on desired behavior. Due to DTPF similarities to STPF it inherits the possibility of resonance problems [13].

#### 2.3.1.2 High-Pass Filter

High-pass filters (HPF) attenuate higher-order harmonics over a wide frequency range but their low selectivity makes them less effective for dominant low-order harmonics, which often require tuned filters for adequate mitigation, Fig. 2.7.

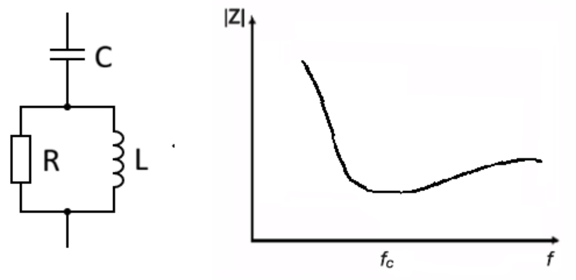


**Figure 2.7:** Configuration of a HPF and its characteristic impedance with components labeled

The cutoff frequency ($f_c$) determines the filters operating range for $f \gg f_c$ the signal passes, while for $f \ll f_c$ the signal is blocked. The cutoff frequency is determined by the resonance of a LC circuit (2.11). HPF are commonly used in power systems to attenuate higher-order harmonic components. This is achieved by providing a low-impedance path for harmonic currents allowing them to be shunted away from the system where the fundamental frequency component experiences high impedance and therefore does not flow through the filter. Quality factor of the HPF is defined as

$$Q_F = \frac{R}{\sqrt{LC}} \tag{2.14}$$

and typically in the range of $0.5 < Q_F < 2$ [12][2].

#### 2.3.1.3 C-Type Filter

C-type passive filters (CTPF) reduce losses at the fundamental frequency compared to conventional high-pass filters making them more suitable for high-power applications where efficiency is critical. However this comes at the expense of increased circuit complexity.

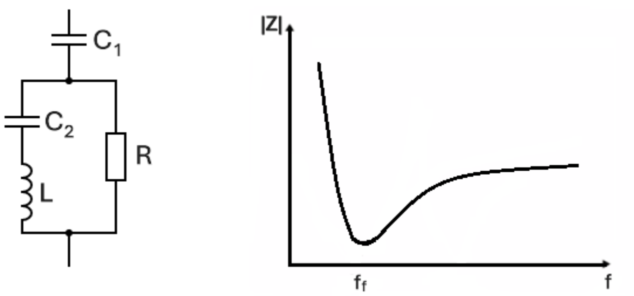


**Figure 2.8:** Configuration of a C-Type high pass filter and its typical characteristic impedance over frequencies with components labeled

At frequencies above the resonance frequency the LC branch is no longer in resonance and its impedance increases. As a result the resistor provides damping. This damping characteristic is essential for maintaining stable operation and avoiding unwanted interactions with the network impedance. In power system applications, C-type filters are commonly used in medium- and high voltage networks where efficiency is an important concern. The quality factor of the CTPF is defined as

$$Q_F = \frac{R}{\omega_r L} \tag{2.15}$$

and typically in the range of $1 < Q_F < 3$ [12][14].

### 2.3.2 Active Harmonic Filters

Active harmonic filters (AHF) are power electronic systems that can filter out harmonic currents by actively detecting and mitigating them in real time. Unlike PHF, AHF use power electronic converters and digital control systems to dynamically inject currents, reducing harmonic distortion and improving power factor. Primary advantage over PHF is their adaptive capabilities. Since the system is controlled electronically, load conditions are continuously monitored making it possible to mitigate harmonic responses in real-time. Unlike PHF, AHF does not possess the risk of operating in resonance with the network. However, these advantages make AHF far more complex and as such, expensive in contrast to PHF [15].

#### 2.3.2.1 Hybrid Active Filter

Hybrid Active Filter (HAF) combine PHF and AHF in order to achieve effective harmonic mitigation with the intent of keeping cost and power rating requirements to a reasonable level. In a hybrid configuration PHF are usually used to target dominant low order harmonics where as the AHF targets the rest and improves PF.[16]

# 3

# Methods

## 3.1 System Modeling in PLECS

PLECS is used as the primary simulation tool due to its suitability for modeling power electronic systems. It provides efficient time-domain simulation of switching devices such as thyristors, while maintaining reasonable computational efficiency. Compared to more general simulation environments, PLECS offers built-in components and analysis tools specifically tailored for power electronics including harmonic analysis.

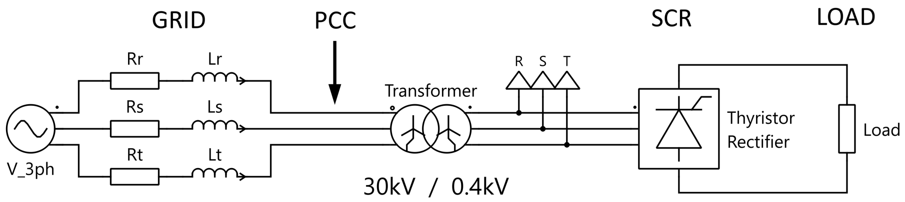


**Figure 3.1:** System overview in PLECS

### 3.1.1 Simulation Conditions

All simulations were performed with consistent operating conditions to ensure comparability between the system configurations.

Grid voltage was set to $30kV$ Line-Neutral at a frequency of $50Hz$. LV side was transformed down to $400V$ using a $75:1$ winding in the transformer. Transformers possessed realistic leakage inductance values and negligible resistance. The firing angle was either kept constant $\alpha = 0°$ and load power adjusted through the load or firing angle was adjusted to obtain desired load power. Both cases of adjusted and constant firing angle was examined due to manufacturers ability to control power by both firing angle in rectifiers and by tap changer in transformers. The two possible strategies are complementary where tap changer control is primarily used to reduce firing angle.

Three different grid strengths were considered, defined by the ratio $\mathrm{I}_{SC}/I_L$ in accordance with IEEE 519, representing different grid strengths and thereby different requirements.

Each simulation was run for sufficient time to reach steady-state conditions before measurements of THD, TDD and power factor were performed at the point of common coupling (PCC).

### 3.1.2 Grid

The grid was represented by an equivalent Thevenin model consisting of a series resistance and inductance. This approach captures the frequency-dependent impedance of an upstream network while maintaining a simple and efficient representation. The values of the resistance and inductance were selected to reflect different grid strengths defined by the ratio of short-circuit current to load current ($I_{SC}/I_L$) in accordance with IEEE 519 requirements in table 2.2. With the intent of investigating different levels of requirements appropriate values $I_{SC}$ in the grid of 5kA, 10kA and 20kA is assumed. with and $X/R$ ratio of 15 [17]. This should produce an $I_{SC}/I_L$ ratio of approximately 40, 80 and 160 in the 5MW systems and sub 20 in the 50MW systems. By varying these parameters, different requirements could be examined.

### 3.1.3 Harmonic Filters

In this work established passive filters (STPF, DTPF, CTPF and HPF) are selected due to their relative simplicity, robustness and widespread industrial application. These characteristics make passive filters suitable for high-power applications.

### 3.1.4 Multi-pulse Thyristor Rectifier

Multi-pulse thyristor rectifier configurations (6, 12, and 24-pulse) were selected for this study based on industrial relevance and project scope defined in collaboration with KraftPowercon. These configurations represent commonly used solutions for high-power rectification where increasing pulse number is a well established method for reducing harmonic distortion.

By including 6, 12, and 24-pulse systems the study captures different levels of harmonic mitigation, allowing a consistent evaluation of how filtering requirements and performance vary with rectifier topology.

The load for the rectifiers are modeled as a resistive-inductive (RL) branch with a minor parallel capacitance. The resistive component represents the active power consumption while the inductive component captures the typical behavior of industrial loads and contributes to a more realistic current waveform.

A minor parallel capacitance is included based on observations provided by KraftPowercon indicating that practical systems exhibit capacitive effects. This load representation provides a simplified yet realistic approximation of industrial operating conditions while maintaining numerical stability in the simulations.

## 3.2 Simulation Setup

### 3.2.1 Multi-pulse Thyristor Rectifiers

Simulation of a 6-pulse rectifier in PLECS can be implemented in two ways, as shown in Fig. 3.2.

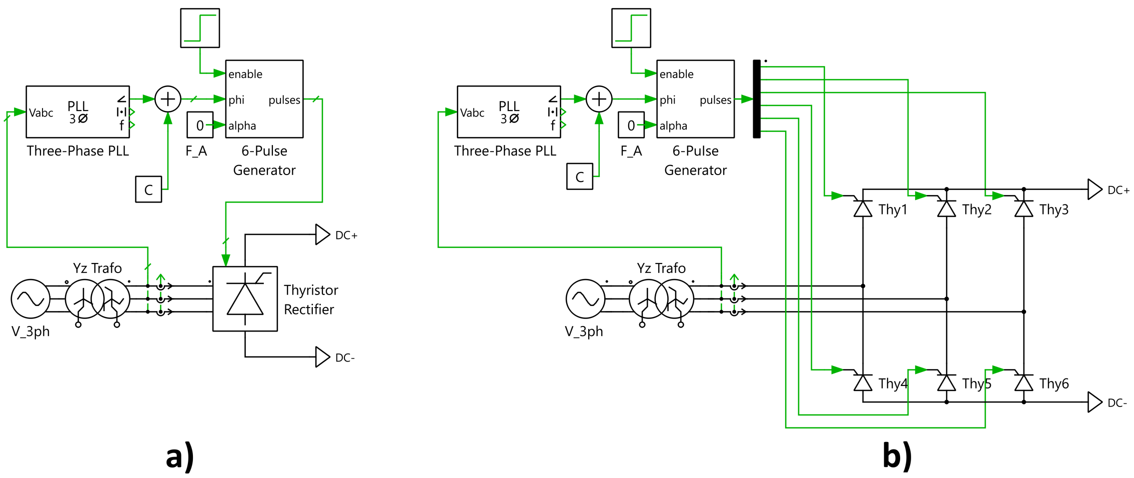


**Figure 3.2:** 6-pulse Thyristor Rectifier in PLECS using a) pre-made rectifier block b) individual thyristors

For lower pulse configurations individual thyristors were used in order to provide a clearer understanding of the operation and switching behavior.
For higher pulse configurations such as the 24-pulse rectifier, the pre-made rectifier block was used to simplify the model and reduce complexity.

Y-Z transformers were used due to the precise ability to easily implement specific phase shifts in simulations. For the 12-pulse system, phase shift was 0°, +30°, and for 24-pulse ±7.5, ±22.5 to reflect realistic systems. A 3-phase meter was then connected after the transformer on the LV side.

Using a 3-Phase meter connected to the 6-Pulse Generator through the PLL, as seen in Fig. 3.2, a reference error occurs creating the need for an added constant (C), the reference error offsets firing angle $\alpha$ (F_A) and varies dependent on chosen measuring metric, Line-Line or Line-Neutral, Fig. 3.3

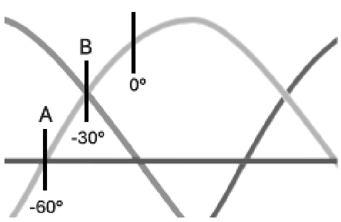


**Figure 3.3:** Part of three-phase curve and reference error for Line-Neutral (A) and Line-Line (B) measurement from intended 0°

For Line-Neutral measurement the constant (C) is set to 60° and for Line-Line measurement 30° to ensure the operating properties $\alpha = 0°$.
The load-power is determined by the resistance of the load resistor

$$R_{load} = \frac{U_{DC}^2}{P_{ref}} \tag{3.1}$$

and is calculated using logical operators and measurements in PLECS. Once steady state was achieved at 100% power of a system the dynamic load is locked into a static state, enabling variation of firing angle and therefore operation at $< 100\%$ using firing angle.

### 3.2.2 Harmonic Filters

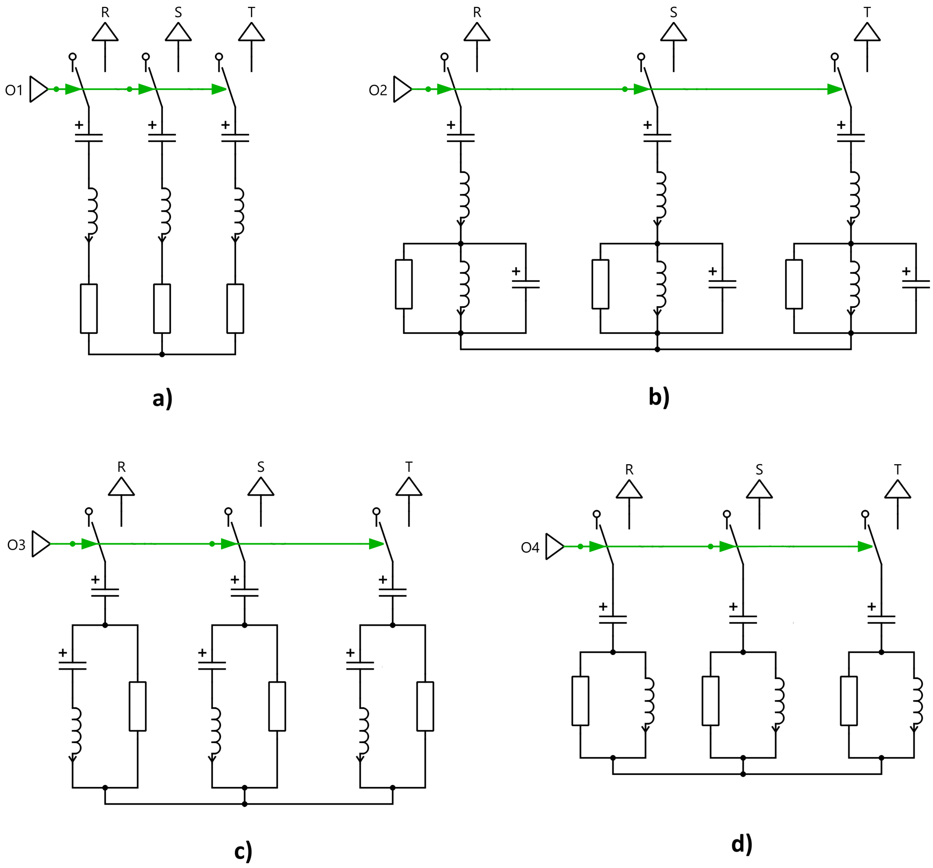


**Figure 3.4:** Configuration of a) STPF b) DTPF c) CTPF d) HPF used in PLECS simulation connected to the three phases R, S and T.

Note that a switch is connected between all filter branches and the three phases R, S and T, the switch is controlled by a signal (O1, O2, O3 and O4). This is done to improve usability by eliminating the need for constant re-modeling when testing different filter combinations.

In case of multi-pulse configurations with multiple three-phase branches on the LV side, identical filters were used on each branch.

## 3.3 Component Dimensioning

### 3.3.1 Transformer Parameters

The relation between the primary and secondary transformer voltage is determined by the winding ratio

$$\frac{V_1}{V_2} = \frac{N_1}{N_2} \tag{3.2}$$

where $V_1$ and $V_2$ are the primary and secondary voltages and $N_1$, $N_2$ is the number of windings. Using the transformer relation (3.2), the MV of 30 kV at PCC ($V_1$) and the rectifier feeding voltage of 400 V ($V_2$) is used to determine the winding relation ($N_1 : N_2$) of the transformers used in modeling to be

$$\frac{30 \cdot 10^3}{400} = \frac{75}{1} \tag{3.3}$$

Base impedance of one transformer is determined by voltage and apparent power at one transformer

$$Z_{base} = \frac{V_{LL}^2}{S} \tag{3.4}$$

and can be used in the calculation of short-circuit impedance. For power transformers the short-circuit impedance ($Z_{sc}$) typically ranges between 4-6% and is mainly dominated by the transformers leakage inductance [18]. The leakage inductance can therefore be estimated to

$$L = \frac{Z_{sc}}{\omega} \tag{3.5}$$

Due to practicality in determining appropriate values for transformer leakage inductance for each load a PF of 1 is assumed, therefore $S = P$ and short circuit impedance to be 4%. The leakage inductance for one of the two windings in the transformer can therefore be calculated

$$L_{leakage} = \frac{0.04V_{LL}^2}{2P\omega} \tag{3.6}$$

**Table 3.1:** Calculated leakage inductance values for one transformers Primary/Secondary winding at different load and topologies, configurations with marked X not examined

| Load (MW) | 6-pulse | 12-pulse | 24-pulse |
|---|---|---|---|
| 5 | $34mH/6.1\mu H$ | $69mH/12.3\mu H$ | $138mH/24.5\mu H$ |
| 50 | X | X | $13.8mH/2.5\mu H$ |

The IPR is approximated (2.8) to be $0.001H$ in 5MW systems and $0.0001H$ in 50MW systems.

### 3.3.2 Grid Dimensioning

Investigated grid strength is divided into three sections. The levels are based of SCC/IL values in Table. 2.2.
For the purpose of this report, grid strength is defined as

$$\frac{I_{SC}}{I_L} \tag{3.7}$$

in accordance to table 2.2 where $I_L$ is the maximum load current, and $I_{SC}$ the grid short circuit current. Short circuit current is chosen to values of 5kA, 10kA and 20kA, the grid equivalent impedance can be calculated as

$$Z_{grid} = \frac{V_{LL}}{\sqrt{3}I_{SC}} \tag{3.8}$$

After selecting an appropriate X/R ratio (15), the line resistance and line reactance can then be calculated using

$$Z_{grid} = \sqrt{R_{grid}^2 + X_{grid}^2} \tag{3.9}$$

and the inductance of the grid is calculated as

$$L = \frac{X}{\omega} \tag{3.10}$$

This gives

$$R = \frac{Z}{\sqrt{1+k^2}} \tag{3.11}$$

$$L = \frac{Zk}{\omega\sqrt{1+k^2}} \tag{3.12}$$

where k = X/R ratio.

### 3.3.3 Filter Dimensioning

For a three-phase system connected in a star configurations the per phase quantities are calculated as

$$Q_\phi = \frac{Q}{3} \qquad V_\phi = \frac{V_{LL}}{\sqrt{3}} \tag{3.13}$$

using this relations the per phase reactance at the fundamental frequency becomes

$$X_{50} = \frac{V_\phi^2}{Q\phi} \tag{3.14}$$

In order to achieve desired PF the compensation is to be based of the reactive effect of the load

$$Q_L = P(tan(cos^{-1}(PF)) \tag{3.15}$$

and required reactive effect of a harmonic filter can therefore be calculated as

$$Q_C = P(tan(cos^{-1}(PF_{current})) - tan(cos^{-1}(PF_{wanted}))) \tag{3.16}$$

In case of multiple filters connected at the same point of coupling, $Q_c$ is divided among the filters used according to the amplitude of the target harmonic

$$Q_{C,h} \approx \frac{I_h}{\sum I_h} Q_C \tag{3.17}$$

This produces an approximate initial sizing and distribution in multiple filters while final distribution may require adjustments. Since 6-24-pulse systems are based on a singular or multiple 6-pulse branches the harmonics amplitude relations of a system can be assumed to be similar to that of a 6-pulse branch at the system specific harmonics (2.4).

#### 3.3.3.1 Single Tuned Passive Filter

The dimensioning of capacitor for the single tuned filter is based on the required filter bank VAr to obtain acceptable power factor

$$C = \frac{Q_C}{3\omega V_\phi^2} \tag{3.18}$$

The inductor is then dimensioned (2.11) to resonate with the capacitor at desired harmonic frequency

$$L = \frac{1}{\omega_h^2 C} \tag{3.19}$$

where as the resistor is chosen with regards to the filters quality factor

$$R = \frac{\omega_h L}{Q_F} \tag{3.20}$$

with a chosen $Q_F$ of 50. The quality factor can be adjusted to achieve desired behavior of the filter.

#### 3.3.3.2 Double Tuned Passive Filter

Due to the combined series and parallel structure of a DTPF, as seen in Fig. 2.6 the component interactions become more complex than a STPF. The DTPF targeting harmonics $x$ and $y$ can therefore be calculated as two STPF targeting harmonics

$x$ and $y$. The series resonance frequency ($\omega_s$) and the parallel resonance frequency ($\omega_p$) behavior of the DTPF can be described as

$$\omega_s = \frac{1}{\sqrt{L_1C_1}} \qquad \omega_p = \frac{1}{\sqrt{L_2C_2}} \tag{3.21}$$

and $\omega_a$, $\omega_b$ the resonance frequencies of the two STPF with targeted harmonics, where

$$\omega_a\omega_b = \omega_s\omega_p \tag{3.22}$$

$C_1$ is obtained as the sum of capacitance used in the STPF (3.18)

$$C_1 = C_{STPF(a)} + C_{STPF(b)} \tag{3.23}$$

and the relation

$$C_1\frac{1}{\omega_p^2} = C_{STPF(a)}\frac{1}{\omega_b^2} + C_{STPF(b)}\frac{1}{\omega_a^2} \tag{3.24}$$

is used where

$$L_1 = \frac{1}{C_{STPF(a)}\omega_a^2 + C_{STPF(b)}\omega_b^2} \tag{3.25}$$

is obtained to achieve series resonance in the DTPF [19]. The parallel resonance in the filter

$$\omega_p = \frac{\omega_a\omega_b}{\omega_s} \tag{3.26}$$

is used to determine

$$L_2 = \frac{(1-\frac{\omega_a^2}{\omega_s^2})(1-\frac{\omega_a^2}{\omega_p^2})}{C_1\omega_a^2} \tag{3.27}$$

where finally $C_2$ can be obtained to achieve the DTPF parallel resonance [19]

$$C_2 = \frac{1}{L_2\omega_p^2} \tag{3.28}$$

The resistance is then chosen to an appropriate value to achieve desired behavior.

#### 3.3.3.3 High-Pass

The HPFs simple design components are directly calculated using the formula for resonance frequency in a LC circuit (2.11) where the capacitor is calculated using the required filter bank

$$C = \frac{Q_C}{3\omega_1V_\phi^2}. \tag{3.29}$$

The inductance is then decided as

$$L = \frac{1}{\omega_c^2C} \tag{3.30}$$

where R is calculated using the quality factor $0.5 < Q_F < 2$

$$R = Q_F\sqrt{LC}. \tag{3.31}$$

#### 3.3.3.4 C-Type

Capacitor $C_1$ in figure 2.8 is calculated as

$$C_1 = \frac{Q_c}{3\omega V_\phi^2} \tag{3.32}$$

and $C_2$ as

$$C_2 = C_1(h_t^2 - 1) \tag{3.33}$$

Inductor L is then chosen for resonance at the fundamental frequency with $C_2$

$$\omega_f L = \frac{1}{\omega_f C_2} \Rightarrow L = \frac{1}{\omega_f^2 C_2} \tag{3.34}$$

R can then be decided with a desired quality factor as

$$R = Q_F \omega_h L. \tag{3.35}$$

# 4

# Results

## 4.1 Basic Operation of Thyristor Rectifiers

The unfiltered values for the 6-, 12- and 24-pulse rectifier is presented in Table. 4.1.

**Table 4.1:** Unfiltered values 6-24-pulse rectifier 5 MW, *load by firing angle

| Config | $P_{Load}$ (%) | TDD (%) | PF | TDD (%)* | PF* |
|---|---|---|---|---|---|
| 6-pulse | 20 | 6.8 | 0.902 | 18.2 | 0.381 |
| | 40 | 13 | 0.922 | 24.9 | 0.555 |
| | 60 | 18.4 | 0.923 | 29.4 | 0.689 |
| | 80 | 23.6 | 0.916 | 31.8 | 0.801 |
| | 100 | 28.5 | 0.909 | 28.5 | 0.909 |
| 12-pulse | 20 | 2.7 | 0.835 | 8.3 | 0.371 |
| | 40 | 5.1 | 0.917 | 10.5 | 0.553 |
| | 60 | 6.4 | 0.934 | 12 | 0.698 |
| | 80 | 7.5 | 0.938 | 12.4 | 0.819 |
| | 100 | 7.6 | 0.936 | 7.6 | 0.936 |
| 24-pulse | 20 | 0.8 | 0.926 | 3.9 | 0.387 |
| | 40 | 1.8 | 0.958 | 5.8 | 0.574 |
| | 60 | 3.3 | 0.957 | 5.9 | 0.717 |
| | 80 | 5.4 | 0.952 | 5.2 | 0.837 |
| | 100 | 6.3 | 0.946 | 6.3 | 0.946 |

The 6-pulse rectifier produce the highest TDD values and lowest PF values among the three configurations. The 12-pulse presents lower TDD and higher PF compared to the 6-pulse and the 24-pulse presents the lowest TDD and the highest PF. TDD and PF are presented in two ways, system configured to $P_{Load}$ with $\alpha = 0°$ and *system configured to $P_{Load}$ by $\alpha$.

The harmonic content of a unfiltered 6-pulse branch is presented in Fig. 4.1 with the amplitudes in Table. 4.2.

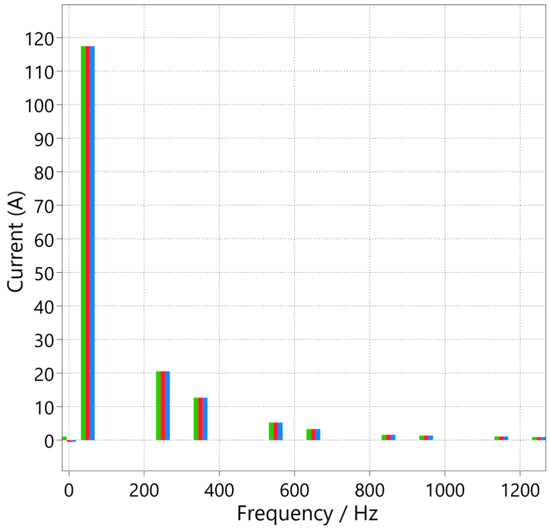


**Figure 4.1:** Harmonic current at PCC in a 6-pulse rectifier branch at 5MW load, colors represent the three phases R, S and T

**Table 4.2:** Harmonic content at PCC in 6-pulse rectifier branch, 5MW load

| Harmonic: | 1 | 5 | 7 | 11 | 13 | 17 | 19 | 23 | 25 | 29 | 31 |
|---|---|---|---|---|---|---|---|---|---|---|---|
| Amplitude: | 117.4 | 20.34 | 12.43 | 4.96 | 3.0 | 1.47 | 1.29 | 1.05 | 0.86 | 0.4 | 0.2 |

Cases of reactive power needed in dimensioning of a PHF for PF correction (3.16) is illustrated in Fig. 4.2.

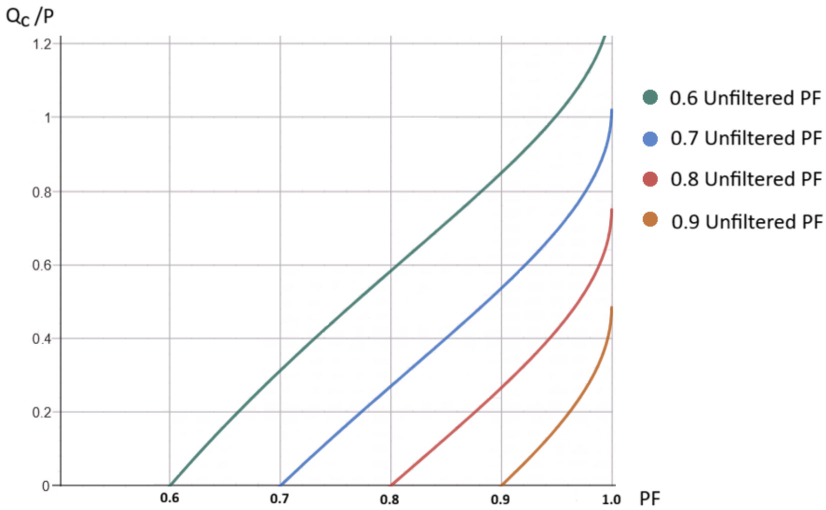


**Figure 4.2:** Equation 3.16 illustrated, comparing filter size to load size ($Q_C/P$) required for reaching equivalent PF

The illustrated theoretical equation shows how reactive compensation required to achieve desired PF becomes significantly larger when unfiltered PF is lower or desired PF is close to 1. The graph indicates that for a unfiltered system with a PF of 0.6

to achieve a PF of 0.95, the required reactive compensation is as large as the load of the system.

## 4.2 Filter Evaluation

Simulations were performed under 2 conditions; variable load with fixed firing angle (0°) and variable load by firing angle. Variation with fixed firing angle, represents a smaller load than rated and can give some estimates of how control strategies such as a tap changer can come to influence the harmonic distortion.

Case 1-4 was examined at a grid strength with $I_{SC} = 10kA$ but rough comparisons can be made across IEEE519 limits imposed by $I_{SC} = 5 - 20kA$ in 5MW systems due to results in table 4.13.

### 4.2.1 Case 1: 6-pulse Thyristor Rectifier, 1-5MW, Passive Filtering

Passive harmonics filtering for Case 1 was accomplished using 2x Single Tuned Passive Filter and 1x C-type High Pass filter, with a total reactive power bank of 2400kVAr. The 2x STPFs target 5th and 7th harmonic with the CTPF targeting higher harmonics.

To maintain both acceptable power factor and %TDD for different load conditions, the filters are switched on in stages. For <3MW load power, the filter bank is sized to 680kVAr, with the remaining reactive power added on for >3MW load power. At low load conditions (<2MW), the C-type filter is disconnected entirely to maintain power factor.

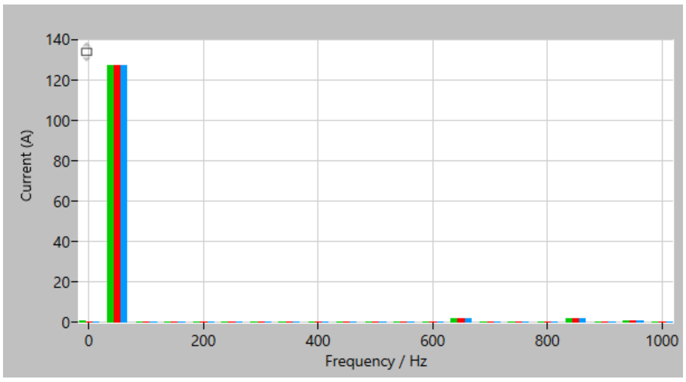


**Figure 4.3:** Harmonic current at PCC current after targeting 5th and 7th harmonic with two single tuned passive filter and a C-type high pass filter, 6-pulse rectifier at 5MW load, $\alpha = 0$, colors represent the three phases R, S and T

With the system configured to $P_{Load}$ with $\alpha = 0°$, TDD and PF is presented against load in Table. 4.3, TDD against load is illustrated in Fig. 4.4 and PF against load is illustrated in Fig. 4.5.

**Table 4.3:** Table of Load Power, %TDD, and Power factor with fixed firing angle $\alpha = 0°$

| $P_{Load}$ (%) | TDD (%) | PF |
|---|---|---|
| 20 | 4.2 | 0.98 |
| 40 | 3.4 | 0.987 |
| 60 | 4.8 | 0.988 |
| 80 | 3.9 | 0.982 |
| 100 | 4.8 | 0.987 |
| | | |

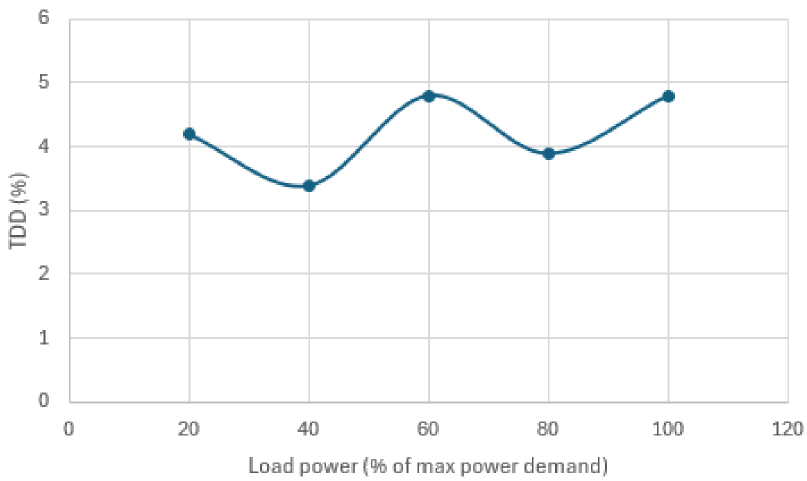


**Figure 4.4:** Graph of %TDD plotted against load power, with fixed firing angle $\alpha = 0°$

The shape of the curve is explained by the staged filters. The filters provided efficient harmonic mitigation and the remaining distortion levels are well below IEEE 519 limits under fixed-firing angle operation.

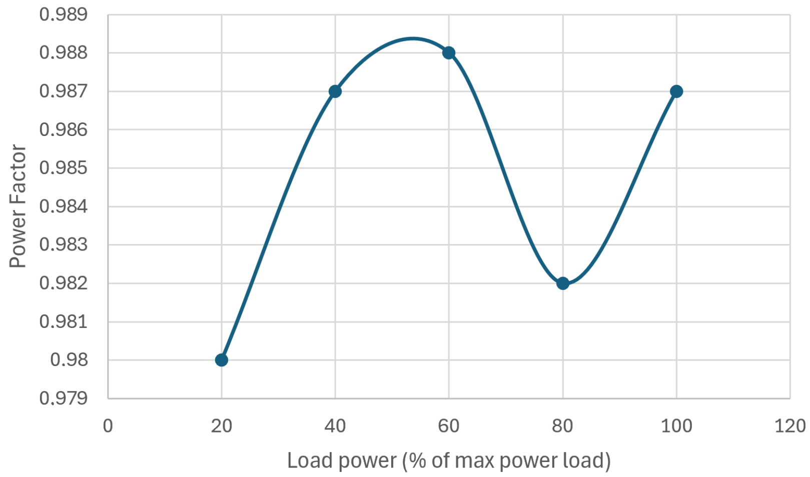


**Figure 4.5:** Graph of power factor plotted against load power, with fixed firing angle $\alpha = 0°$

The large filter bank provides great reactive compensation and a PF above 0.98 is achieved during all loads under fixed-firing angle operation.

With the system configured to $P_{Load}$ by $\alpha$, TDD and PF is presented against load and $\alpha$ in Table. 4.4, TDD against load is illustrated in Fig. 4.6 and PF against load is illustrated in Fig. 4.7.

**Table 4.4:** Table of load power, %TDD, power factor and firing angle.

| $P_{Load}$ (%) | TDD (%) | PF | Firing Angle (°) |
|---|---|---|---|
| 20 | 5.8 | 0.538 | 63 |
| 40 | 7.8 | 0.692 | 51 |
| 60 | 8.8 | 0.811 | 39 |
| 80 | 6.7 | 0.955 | 27 |
| 100 | 4.7 | 0.978 | 0 |

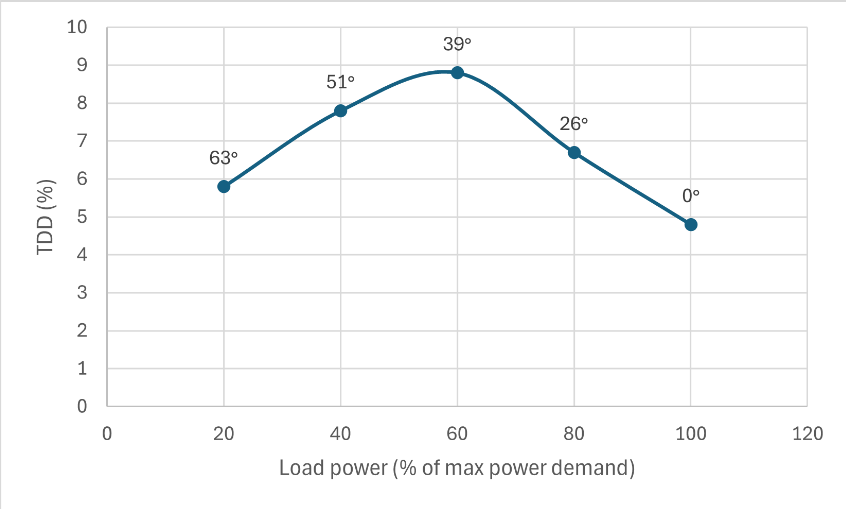


**Figure 4.6:** Graph of %TDD against load power, where firing angle varies depending on load demand.

When introducing firing angle TDD increases notably due to the worsened harmonic distortion caused by the firing angle.

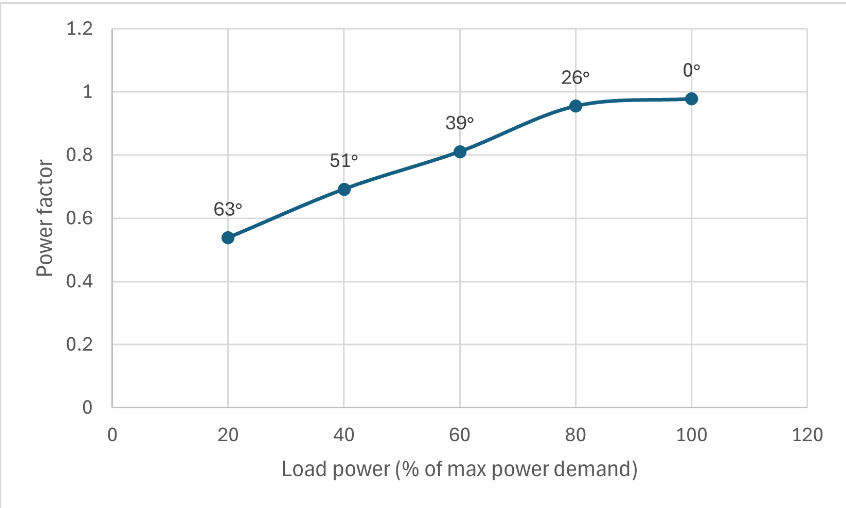


**Figure 4.7:** Graph of power factor against load power, where firing angle varies depending on load demand.

PF decreases significantly as the firing angle increases.

### 4.2.2 Case 2: 12-pulse Rectifier, 1-5MW, Passive Filtering

Passive harmonics filtering for Case 2 was accomplished using 2x STPFs targeting the 11th and 13th harmonics. Total filter bank reactive power is 423 kVAr.

As with Case 1, simulations were performed under fixed firing angle condition and variable firing angle condition.

**Table 4.5:** Table of load power, %TDD, and power factor with fixed firing angle $\alpha = 0°$. 12-pulse, 5MW.

| $P_{Load}$ (%) | TDD (%) | PF |
|---|---|---|
| 20 | 0.7 | 0.988 |
| 40 | 1 | 0.994 |
| 60 | 1.2 | 0.985 |
| 80 | 1.3 | 0.973 |
| 100 | 1.3 | 0.957 |

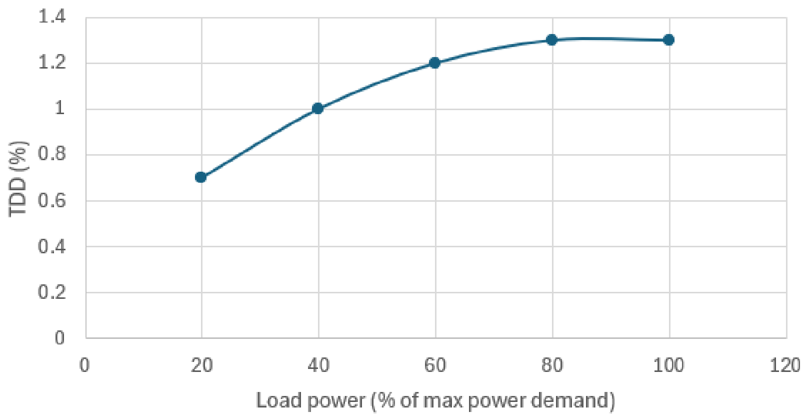


**Figure 4.8:** Graph of %TDD plotted against load power for a 5MW rated 12-pulse rectifier, with fixed firing angle $\alpha = 0°$.

The 12-pulse configuration achieved substantially lower TDD compared to the 6-pulse system due to harmonic cancellation. The remaining distortion levels were well below IEEE 519 limits under fixed firing-angle operation.

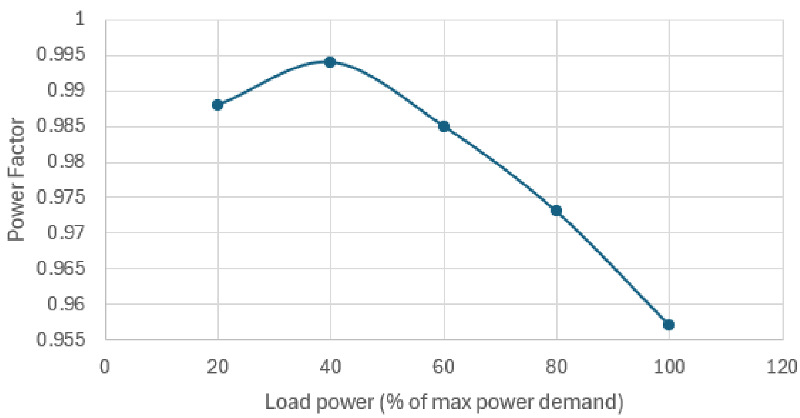


**Figure 4.9:** Graph of power factor plotted against load power for a 5MW rated 12-pulse rectifier, with fixed firing angle $\alpha = 0°$

PF at 100% load is lower than the 6-pulse configuration due to the filter bank being configured to target a lower PF. At approximately 30% load power, overcompensation occurs and PF decreases at lower load power.

**Table 4.6:** Table of load power, %TDD, power factor and firing angle for a 12-pulse 5MW rated rectifier.

| $P_{Load}$ (%) | TDD (%) | PF | Firing Angle (°) |
|---|---|---|---|
| 20 | 1.2 | 0.405 | 63 |
| 40 | 2.46 | 0.594 | 51 |
| 60 | 3.15 | 0.740 | 39 |
| 80 | 3.18 | 0.862 | 26 |
| 100 | 1.33 | 0.956 | 0 |

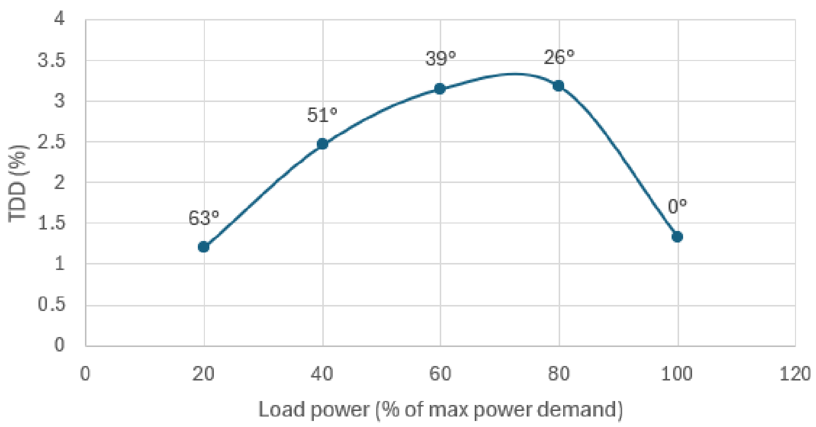


**Figure 4.10:** Graph of %TDD plotted against load power for a 5MW rated 12-pulse rectifier, with varying firing angle. Firing angle is presented for each data point.

With firing angle dependency the 12-pulse system still manages TDD values far below IEEE 519 limits.

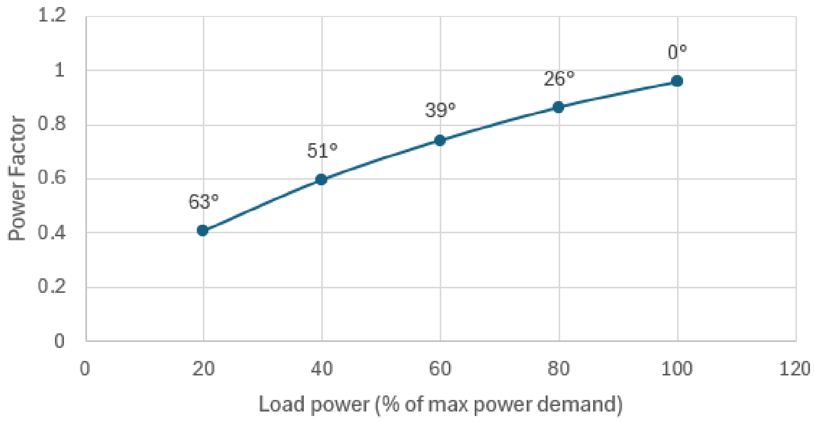


**Figure 4.11:** Graph of power factor plotted against load power for a 5MW rated 12-pulse rectifier, where firing angle varies depending on load demand. Firing angle is presented for each data point.

PF decreases significantly as the firing angle increases.

### 4.2.3 Case 3: 24-pulse Rectifier, 1-5MW, Passive Filtering

Passive harmonics filtering for Case 3 was accomplished using 1x HPF per phase shift targeting the 23th harmonic and above. Total filter bank reactive power is 874kVAr.

**Table 4.7:** Table of load power, %TDD, and power factor with fixed firing angle $\alpha = 0°$. 24-pulse, 5MW rated rectifier.

| $P_{Load}$ (%) | TDD (%) | PF |
|---|---|---|
| 20 | 0 | 0.954 |
| 40 | 0.1 | 0.987 |
| 60 | 0.3 | 0.988 |
| 80 | 0.5 | 0.983 |
| 100 | 0.6 | 0.975 |

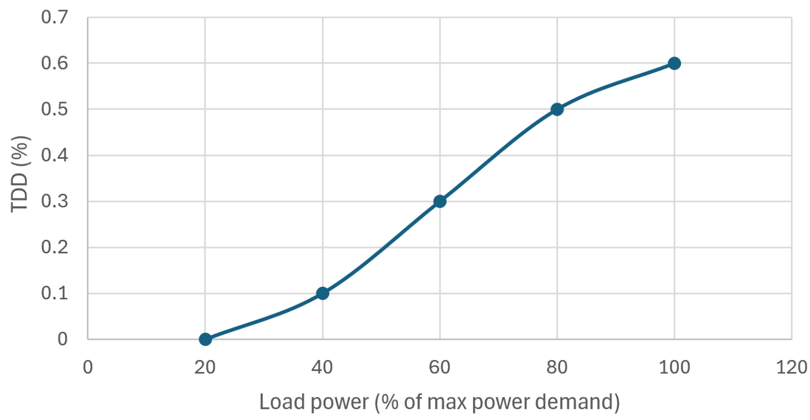


**Figure 4.12:** Graph of %TDD plotted against load power for a 5MW rated 24-pulse rectifier, with fixed firing angle $\alpha = 0°$

The 24-pulse achieves excellent values on TDD under fixed firing-angle operation using a simple HPF, with remaining distortion levels far below limits specified in IEEE 519.

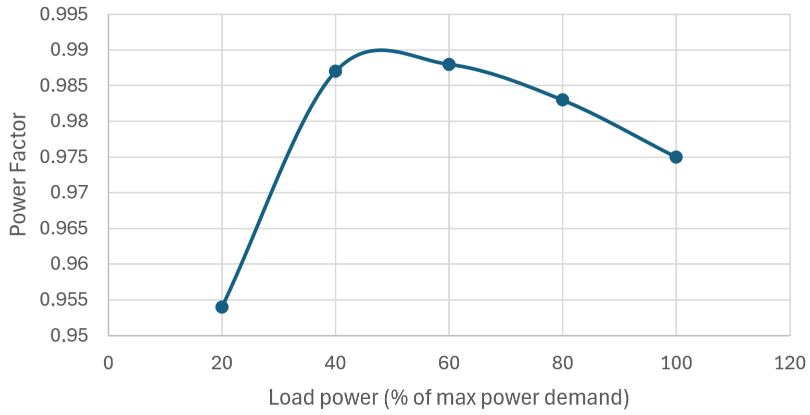


**Figure 4.13:** Graph of power factor plotted against load power for a 5MW rated 24-pulse rectifier, with fixed firing angle $\alpha = 0°$

PF at 100% load is higher than the 12-pulse configuration due to the configured filter bank targeting a higher PF. Consequently, overcompensation occurs earlier in the operating range. The load power at which overcompensation occurs can be obtained when the reactive filter compensation (3.16) exceeds the reactive effect by the load (3.15), this can be expressed as

$$k = \frac{Q_C}{P(tan(cos^{-1}(PF))} \cdot 100\% \tag{4.1}$$

where PF is the unfiltered value and P the load at 100%, in this case k = 51%.

**Table 4.8:** Table of load power, %TDD, power factor and firing angle for a 24-pulse 5MW rated rectifier.

| $P_{Load}$ (%) | TDD (%) | PF | Firing Angle (°) |
|---|---|---|---|
| 20 | 0.2 | 0.477 | 63 |
| 40 | 0.7 | 0.651 | 51 |
| 60 | 1.1 | 0.773 | 39 |
| 80 | 1.6 | 0.881 | 26 |
| 100 | 0.6 | 0.975 | 0 |

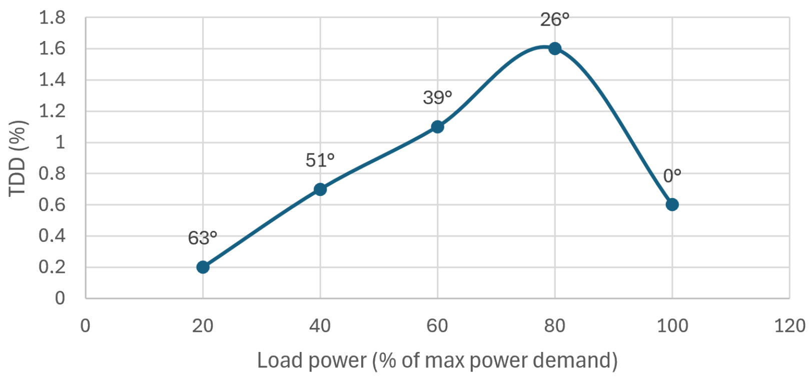


**Figure 4.14:** Graph of TDD plotted against load power for a 5MW rated 24-pulse rectifier, where firing angle varies depending on load demand. Firing angle is presented for each data point.

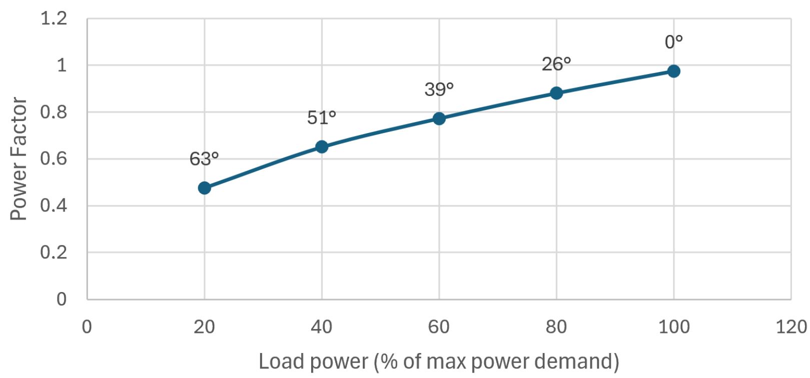


**Figure 4.15:** Graph of power factor plotted against load power for a 5MW rated 24-pulse rectifier, where firing angle varies depending on load demand. Firing angle is presented for each data point.

Using the HPF, TDD is far below IEEE 519 limits even with added firing angle. PF decreases as firing angle increases.

### 4.2.4 Case 4: 24-pulse rectifier, 10-50MW

Passive harmonics filtering for case 4 was accomplished using 1x HPF targeting the 23rd harmonic and above. Total filter bank reactive power is 5.83MVAr.

**Table 4.9:** Table of load power, %TDD, and power factor with fixed firing angle $\alpha = 0°$. 24-pulse, 50MW rated rectifier.

| $P_{Load}$ (%) | TDD (%) | PF |
|---|---|---|
| 20 | 0.3 | 0.97 |
| 40 | 0.6 | 0.992 |
| 60 | 0.8 | 0.995 |
| 80 | 1.6 | 0.994 |
| 100 | 1.9 | 0.992 |

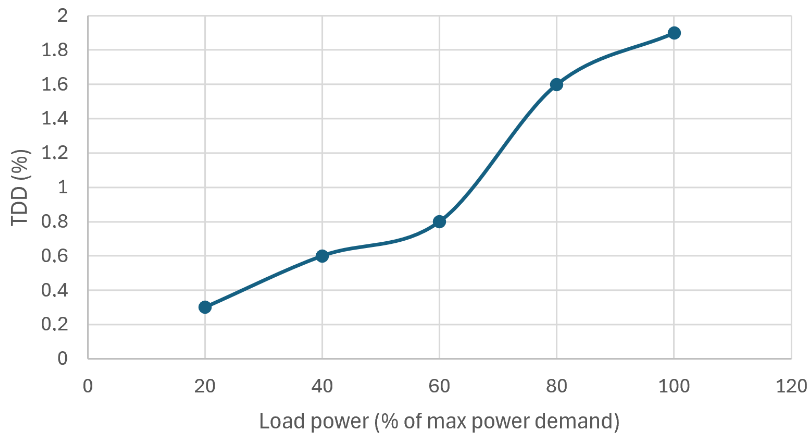


**Figure 4.16:** Graph of %TDD plotted against load power for a 50MW rated 24-pulse rectifier, with fixed firing angle $\alpha = 0°$

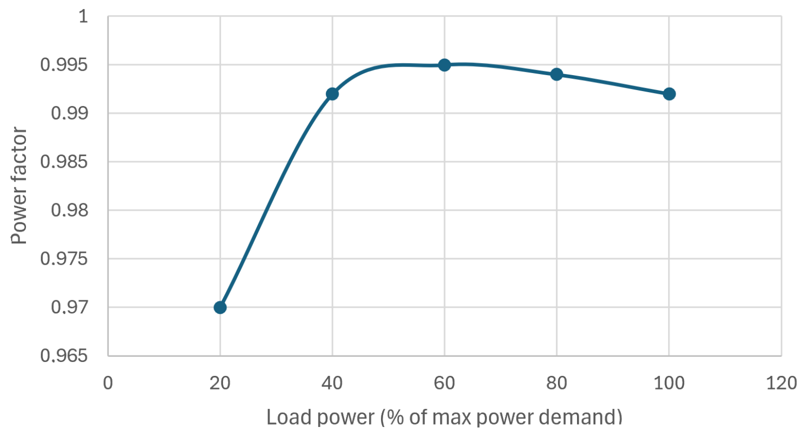


**Figure 4.17:** Graph of power factor plotted against load power for a 50MW rated 24-pulse rectifier, with fixed firing angle $\alpha = 0°$

**Table 4.10:** Table of load power, %TDD, power factor and firing angle for a 24-pulse 50MW rated rectifier.

| $P_{Load}$ (%) | TDD (%) | PF | Firing Angle (°) |
|---|---|---|---|
| 20 | 1.14 | 0.490 | 63 |
| 40 | 1.66 | 0.665 | 51 |
| 60 | 1.86 | 0.797 | 39 |
| 80 | 2.1 | 0.904 | 26 |
| 100 | 1.9 | 0.992 | 0 |

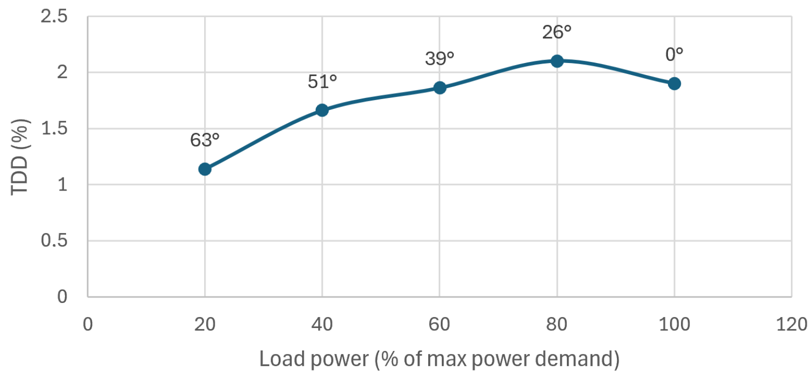


**Figure 4.18:** Graph of %TDD plotted against load power for a 50MW rated 24-pulse rectifier, where firing angle varies depending on load demand. Firing angle is presented for each data point

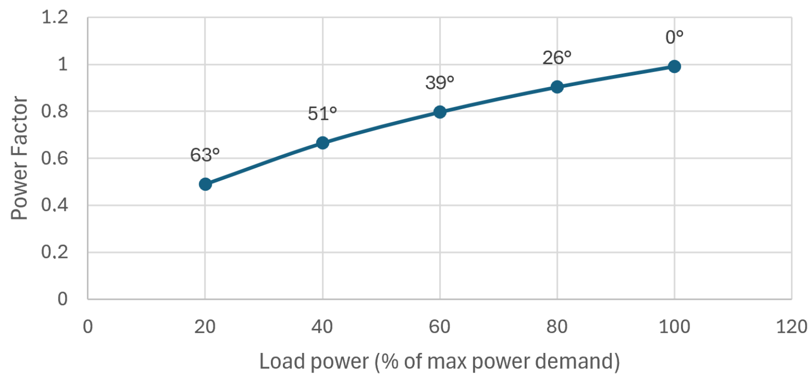


**Figure 4.19:** Graph of power factor plotted against load power for a 50MW rated 24-pulse rectifier, where firing angle varies depending on load demand. Firing angle is presented for each data point

The 24-pulse, 50MW system exhibits values close to those of the 5MW system.

## 4.3 Practical Filter Considerations

The largest unfiltered harmonic current for each rectifier configuration determines the current/power rating of passive filter components, and are presented in fig 4.20. The largest harmonics are the 5th harmonic for the 6-pulse, 11th harmonic for the 12-pulse, and 23rd harmonic for the 24-pulse.

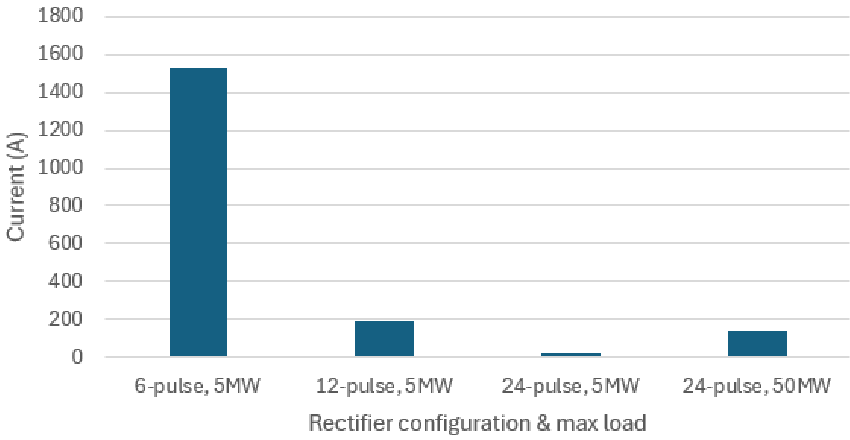


**Figure 4.20:** Largest harmonic for each rectifier configuration.

The substantially larger harmonic current in the 6-pulse, 5MW system is due to the presence of the dominant low-order harmonics and the lack of multiple branches where current is distributed.

Table 4.11 & 4.12 show simulated filter real power as percentage of load power & filter real power to filter reactive power ratio.

**Table 4.11:** Simulated filter real power resistive losses for different configurations at their max load power demand. The fourth column represents real power filter losses as a ratio of the load power.

| Configuration | Simulated filter active power $P_F$ (kW) | Load power $P_{Load}$ (kW) | $P_F/P_{Load}$ |
|---|---|---|---|
| 6-pulse 5MW | 10.1 | 5000 | 0.2% |
| 12-pulse 5MW | 3.57 | 5000 | 0.07% |
| 24-pulse 5MW | 24.7 | 5000 | 0.5% |
| 24-pulse 50MW | 61.4 | 50000 | 0.13% |

**Table 4.12:** Table of simulated filter real power, filter reactive power size, and real power to reactive power ratio.

| Rectifier configuration | Simulated filter active power $P_F$ (kW) | Installed filter Q $Q_F$(kVAr) | $P_F/Q_F$ |
|---|---|---|---|
| 6-pulse 5MW | 10.1 | 2400 | 4.2 W/kVAr |
| 12-pulse 5MW | 3.57 | 423 | 8.4 W/kVAr |
| 24-pulse 5MW | 24.7 | 874 | 28.3 W/kVAr |
| 24-pulse 50MW | 61.4 | 5830 | 10.5 W/kVAr |

### 4.3.1 Grid Resilience

**Table 4.13:** TDD and PF with grid strength in a 5MW and 50MW 24-pulse rectifier with $\alpha = 0°$.

| $P_{Load}$ (MW) | $I_{SC}/I_L$ | TDD(%) | PF |
|---|---|---|---|
| 5 | 163.7 | 6.5 | 0.946 |
| 5 | 81.7 | 6.3 | 0.946 |
| 5 | 40.6 | 6.1 | 0.945 |
| 50 | 16.6 | 5.4 | 0.949 |
| 50 | 8 | 3.9 | 0.946 |
| 50 | 3.9 | 3.0 | 0.928 |

At the 5MW rated systems, grid strength does not significantly impact values of TDD or PF. In the 50MW systems a greater impact can be observed due to the weakness of the grid strength.

**Table 4.14:** $V_{THD}$ content of unfiltered 5MW pulse configurations systems, at 100% load power

| Config | $I_{SC} = 5kA$ | $I_{SC} = 10kA$ | $I_{SC} = 20kA$ |
|---|---|---|---|
| 6-pulse (5MW) | 3.7 % | 1.7 % | 0.8% |
| 12-pulse (5MW) | 2.0% | 0.9% | 0.4% |
| 24-pulse (5MW) | 0.7% | <0.1% | <0.1% |
| 24-pulse (50MW) | 5.6% | 3% | 1.7% |

Lower-pulse configurations and weaker grids show substantially worse TDD values. In 50MW system, $I_{SC} = 5kA$ the THD limit of 5% is failed, indicating that harmonic filtering is required even though TDD limits are passed.

### 4.3.2 Non-Ideal Parameters

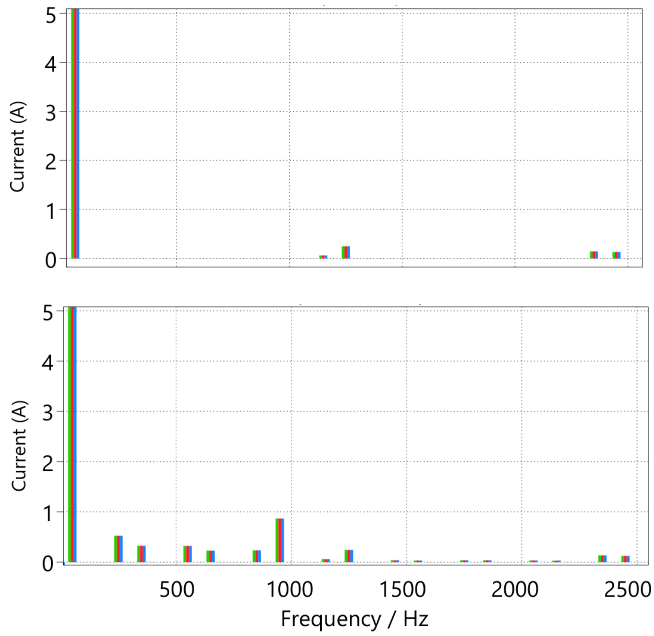


**Figure 4.21:** Harmonic current of a filtered 24-pulse rectifier with ideal phase shift (above) and with non-ideal phase shift (1° offset in one of four transformers, below), colors represent the three phases R, S and T

In the ideal phase shift case TDD was 0.6% TDD, in the non ideal case TDD was 1.9%. The offset of 1° is larger than what can be expected in real implementations but does illustrate problems with non-ideal phase shifts.

# 5

# Analysis and Discussion

## 5.1 Harmonic Distortion Complexity in Thyristor Rectifiers

The results demonstrate that harmonic distortion in thyristor rectifier systems is strongly dependent on pulse configuration, firing angle and operating conditions. Lower pulse configurations generate significantly higher harmonic distortion due to the presence of lower order harmonics. Higher pulse systems reduce harmonic distortion significantly through phase cancellation between rectifier branches.

The simulated 6-pulse rectifier in Fig. 4.1 shows dominant 5th and 7th order harmonics which is consistent with the theoretical harmonic relation (2.4). These low order harmonics showed relatively high amplitudes and therefore contribute heavily to TDD. As a result, the 6-pulse configuration required substantial harmonic filtering in order to comply with IEEE 519 limits. In comparison, the 12-pulse rectifier phase shifts completely mitigates the 5th and 7th order harmonics, and the dominant harmonics were shifted to the 11th and 13th, reducing overall distortion. This resulted in substantially lower TDD values and increased PF which reduced reactive power requirements for the filter bank. The 24-pulse configuration further improves harmonic distortion and PF values using the same working principle as the 12-pulse. As a consequence less filtering is needed.

Even though a clear distinction between the unfiltered pulse-configurations results can be made in the simulations as seen in table 4.1, Kraftpowercons observations of typical unfiltered values distinguishes itself considerably. One possible reason for this, besides non-ideal components, could be transformer leakage settings and parameters which under the project have been observed to have a significant impact on PF and TDD. This impact has not greatly been studied and would require further investigation.

Although increasing pulse number improves harmonic and overall performance, simulations also indicates increasing system complexity can lead to unwanted irregularities.

When regulating load using firing angle PF decreases in relation to lower loads. With firing angles introduced, TDD was not observed to increase significantly in higher pulse systems as can be seen in Fig. 4.10. Although in lower-pulse configurations TDD becomes problematic as can be seen in Fig. 4.6. This behavior is most likely explained by the definition of TDD (2.3), where the harmonic content is normalized using the maximum demand current, rather than the instantaneous operating current. As the load decreases, the harmonic current decreases causing the calculated TDD to remain relatively constant although the actual current waveform distortion worsens. In the 6-pulse rectifier with large amounts of harmonics distortion, the TDD has a greater negative effect than the 12-24 pulse systems where harmonic distortion is less present. The shape of TDD dependent on firing angle can therefore be observed similar across the 6-24 configurations in Fig. 4.6, 4.10 and 4.14, although the numerical values are far inferior in the 6-pulse.

## 5.2 Passive Filter Effectiveness

The simulations demonstrate that PHF can effectively reduce harmonic distortion in thyristor rectifier systems when properly tuned and dimensioned. STPF showed particularly effective attenuation of dominant characteristic harmonics, while CTPF and HPF improved higher order harmonics and reduced TDD. Simulations also provided data for theoretical equations (3.16) where the required reactive filter compensation increases significantly as the difference between unfiltered PF and targeted PF grows. In particular, achieving a PF close to 1 becomes increasingly power intensive as seen in Fig. 4.2.

For the 6-pulse system, an excessive filter bank of 2400kVar was required due to the low unfiltered PF combined with the high target PF. The targeted PF is also the reason for the 24-pulse system requiring a higher effect reactive filter bank than the 12-pulse system where targeted PF was lower.

For the filter bank used in the 6-pulse rectifier system, two STPF were used to target the 5th and 7th harmonics, in addition a CTPF was used to target higher-order harmonics. This still resulted in relatively high TDD values, especially when introducing firing angle. By looking at the 12-pulse filtered system using two STPF to target 11th and 13th harmonic, TDD is significantly improved. This indicates that the 6-pulse system could improve significantly by also targeting 11th and 12th order with targeted harmonic filters such as STPF or DTPF, this would however result in an increase of complexity, size and cost.

In case of the filter system used in the 6-pulse rectifier where targeted PF was close to 1, simulations showed filter bank sizing becoming increasingly sensitive at lower load conditions. At low power operation, the PHF excessive reactive power compensation caused overcompensation making staged switching of the filter bank necessary. Therefore, if a system is designed to operate at a high PF combined with the intent of operating at different load levels, PHF can cause unwanted restraints.

The filters showed effective reduction of harmonics and improvement of PF. However, when operating the system at larger firing angles PF decreases significantly. To counteract this behavior using PHF would require complex switching systems and extensive reactive filter effect. Although systems always aim to operate at close to 0° firing angle under normal operation using a tap changer in the transformer, this will rarely be considered problematic and real implementations could therefore focus more on the operating range.

However, PHFs can become inadequate when non-ideal irregularities appear, one reason for this being the phase shifting used in higher-pulse configurations. The increased pulse bridges require phase shifts, which if not perfectly aligned can lead to lower order harmonics starting to appear even in higher pulse configurations. Figure 4.21 illustrates that a deviation of the phase shift 1° in one out of four transformers is sufficient to introduce previously negligible lower order harmonics. This indicates that higher pulse configurations are highly sensitive to transformer tolerances and asymmetries between the branches. This behavior becomes particularly significant where ideal transformer conditions cannot be guaranteed. As a result PHF design can not completely rely on ideal theoretical harmonic cancellation and should instead consider non-ideal operating conditions. In case of greater irregularities of phase shifting in higher pulse configurations AHF can therefore be of interest.

Another variable not closely examined in this project was the risk of missing targeted harmonics. PHF require precise tuning to operate as intended. In real implementations, exact harmonic location can be non-ideal and exact component values required for ideal resonance are rarely available.

## 5.3 Compliance with IEEE 519

The results show that compliance with IEEE 519 strongly depends on pulse configuration, grid strength and load power. Unfiltered harmonic content of a 6-pulse branch as seen in Fig. 4.1 and table 4.2, can be compared against the TDD requirements table 2.2. This shows that the simulated unfiltered lower-pulse configurations such as 6- and 12-pulse require substantial filters while higher-pulse configurations such as the 24-pulse only struggles at $I_{SC}/I_L < 20$. Table 4.13 therefore indicates that for lower power systems the simulated 24-pulse rectifier passes IEEE 519 requirements without filtering needed, where as the higher power systems require filtering. Lower power systems is able to achieve this due to $I_{SC}/I_L > 20$ individual harmonics as seen in Fig. 4.1, $h > 13$ are able to pass IEEE 519 requirements in table 4 without filtering, whereas individual harmonic requirements $I_{SC}/I_L < 20$ are not fulfilled. Although it is essential to acknowledge that these simulations are far more ideal than real implementations where unfiltered harmonics are liable to worsen values.

Whether or not a system is compliant with IEEE 519 depends heavily on the $I_{SC}/I_L$ ratio. It is demonstrated through the simulations that achieving compliance can be done on even the weakest of grids, as long as the firing angle remains low.

However, varying firing angle increases TDD and in low-pulse systems with large harmonic distortion this can become problematic. Even with extremely heavy filtering, the 6-pulse rectifier reaches unacceptable levels of harmonic distortion, even as the harmonics themselves become smaller. As such, for a multi-MW system which may need quick current regulation through firing angle adjustment, maintaining low TDD with a 6-pulse rectifier becomes unfeasible.

Increasing the size of the rectifier topology quickly solves these issues. With light passive filtering, 12-pulse rectifier remains within compliance even during sudden decreases in load demand and large increases in firing angle. Table 5.1 shows wether each rectifier configuration is below TDD compliance limits during "worst-case" operation (i.e. when %TDD is highest).

**Table 5.1:** IEEE 519 TDD compliance for different grid strength/rectifier configuration combinations, with passive filters. *theoretically

| $I_{SC}/I_L$ | 6-pulse (TDD = 8.8%) | 12-pulse (TDD = 3.18%) | 24-pulse (TDD = 2.1%) |
|---|---|---|---|
| <20 | No* | Yes* | Yes |
| 20 >50 | No | Yes | Yes |
| >50 | Yes | Yes | Yes |

Furthermore, THD values of the system configurations in table 4.14 can be compared to the IEEE 519 requirements seen in table 2.1. It is observed that THD requirements are fulfilled with for all cases except lowest grid strength in the 50MW system. For this case the grid strength defined as $I_{SC}/I_L$ is approximately 4. This indicates that for very weak grids, remaining below the $V_{THD}$ limits may be a larger issue than remaining below the %TDD limits.

## 5.4 Practical implementation considerations

Filtering out harmonics can be effectively done using bandwidth filters connected to the 400V transformer side. For configurations that produce large harmonics, the biggest practical hurdle becomes the need to handle large currents.

Looking at figure 4.20, we see that the RMS current for the 6-pulse 5th harmonic is >1500A. Such large currents inevitably lead to a large build-up of heat in the components. While capacitors are priced competitively at low unit cost even for industrial applications, the filter inductor dimensioning becomes more problematic [20]. In order to effectively filter the targeted harmonic frequency, the inductor must have a low inductance and a high current rating. The inductors current DC resistance, which largely governs copper losses (and current rating) is

$$R_{DC} = \rho \frac{l}{A} \tag{5.1}$$

where $\rho$ is the resistivity of the wire, l its length, and A the cross-sectional area. 5.1 shows that the only way to reduce copper losses is to increase the cross sectional area of the wire, leading to a larger and more expensive inductor. Furthermore, as resistance increases with temperature, very high current inductors may require more than passive cooling, increasing cost & size further. Failing to consider these factors may lead to filter de-tuning or component damage. Combined with the fact that passive filtering for a 6-pulse 5MW rectifier is only slightly below the IEEE 519 %TDD requirements for weak grids, passive filtering may become both prohibitively expensive, phyiscally large, and unsatisfactory. The fact that stage-switched filter banks must be used to maintain acceptable power factor drives cost even further.

In larger configurations, such as the 12-pulse rectifier, passive filtering becomes significantly more practical. With the largest possible harmonics becoming significantly smaller, the necessary current rating of the inductors decreases. Although the required inductance increases slightly as reactive power demand decreases (according to eq. 3.18 & 3.30), this is largely offset by the signifcant reduction in cross sectional area. Inductor current rating requirements drop even further for the 24-pulse 5MW rectifiers, and remains relatively even for the 50MW rated rectifier at maximum load. Given these finding, a clear pattern arises, where passive filtering remains both most unsatisfactory and expensive for 6-pulse rectifiers, more economically and practically viable for 12-pulse rectifiers, and most viable for 24-pulse rectifiers.

## 5.5 Losses & efficiency

Tables 4.11 & 4.12 shows simulated real losses and simulated filter real power in relation to filter reactive power. The 6-pulse filter bank, despite being large at 2400kVAr, has a simulated real power of only 10.1kW. Since most filtering is done by the 5th & 7th harmonic frequency tuned filters, the filter bank is mostly reactive. As such, the filter bank imposes a small efficiency penalty of only 0.2%.

Similairly, for the 12-pulse configuration, the installed filter bank reactive power is small, at 423kVAr. As the filtering here too is done with single tuned filters, and the harmonics are small, the filter bank imposes an efficiency penalty of 0.07%.

The 24-pulse, 5MW configuration is an outlier. With an installed filter capacity of 874kVAr, and a simulated real power of 24.7kW, this filter bank has the highest efficiency penalty and loss per installed kVAr. The 50MW configuration, with a significantly larger filter bank of 5830kVAr, sits at a loss of 10.5W/kVAr and a 0.13% efficiency penalty. Since the harmonic spectrum is identical to the 50MW configuration, a likely explanation is either differences in transformer leakage settings, or that the damping of the 5MW high-pass filter is too aggressive.

It is also important to note that these results should not be interpreted as full physical losses. Since inductors and capacitors are ideal in PLECS, quantities like reactor winding/core loss, busbar loss, skin effects etc. are neglected. Winding losses alone would likely account for a significant portion of real losses, since the inductor must handle kA sized currents in the 6-pulse case. In this scenario, $P_f$ represents the siumulated real power dissipation in the resistive parts of the filter bank.

## 5.6 Sustainability & Ethics

AC/DC rectifiers are a crucial component of electrifying industry, as many industrial applications require high DC currents. As such, rectifiers are an important part of reducing reliance on fossil fuels. Harmonics reduce the power factor and efficiency of rectifiers, leading to a larger input power demand for a similar output power. Effectively filtering these harmonics reduces the amount of "waste power".

Even so, the manufacture of the passive components required for filtering is a highly specialized and resource intensive process. Large amounts of metals must be extracted, materials undergo energy-intensive sintering, and etching and cleaning generates large amounts of wastewater containing heavy metals and other pollutants. Sourcing components from manufacturers that strictly follow environmental regulations is therefore key when considering the sustainability aspect of filter design [21].

Passive electronic components also have a lifespan. Choosing components with long lifespan in mind not only reduces eventual extra costs down the line, but indirectly reduces the environmental impacts. When discarding these components, it is of high importance that this is done responsibly, e.g. through recycling [22].

# 6
# Conclusion

This study investigated harmonic mitigation strategies for high-power thyristor rectifier systems with the objective of achieving compliance with IEEE 519 at PCC. In addition to this practical implementations such as PF, filter size, complexity and system performance were discussed.

The results demonstrate that the pulse number of the rectifier has a major influence on harmonic distortion level and consequently the harmonic filtering required. The 6-pulse rectifier produced the highest harmonic distortion and required extensive passive filtering. Although PHFs proved technically capable of reducing harmonics, the filter complexity and size became unpractical due to high harmonic currents and staged reactive compensation requirements. This makes pure passive harmonic mitigation for high-power 6-pulse rectifiers economically and practically challenging. Instead solutions like a HAF is suiting where PHFs is used to target lower dominant harmonics while providing some reactive compensation and AHF target higher harmonics order and provide final reactive compensation for optimal efficiency.

For the 12-pulse rectifier harmonic amplitudes were significantly reduced compared to the 6-pulse. As a result the system required substantially smaller and more practical filter implementations to meet the requirements set by IEEE 519. However for optimal mitigation, significant filtering is required.

The 24-pulse rectifier system demonstrated the best overall harmonic performance. Due to the negligible low-order harmonic content only limited passive filtering was required to achieve requirements for the weakest grid. This resulted in comparatively small filter currents, leading to lower thermal stress and improved practical feasibility, even for higher power levels. However, these benefits are obtained at the cost of increased transformer and system complexity which in non-ideal implementations can lead to further harmonic distortion complexity.

The study also shows how operation close to a targeted PF of 1 in the rectifier requires increasingly extensive reactive compensation. In case of PHFs this is shown to be increasingly complex as it runs the risk of overcompensating when operating at reduced load, creating the need for staged filters. This would cause the filtering system to scale significantly in size, prize and complexity which consequently could make AHF a more fitting alternative. The need for scaling filters becomes more significant in lower-pulse topologies where the required reactive compensation is larger.

The simulations showed that passive filter losses remained relatively small for the investigated filtering systems. However the simulations performed were close to ideal and real implementations would therefore see significantly greater losses and need to take degradation, inconsistencies and varying operation conditions into consideration. PHF could therefore impose a considerable efficiency penalty in the overall system.

Overall, the work demonstrates that effective harmonic mitigation in high-power thyristor rectifier systems require consideration of both harmonic performance and practical implementation constraints. The result indicate that increasing pulse number is generally more effective and practical than relying solely on extensive passive filtering, especially in high-power industrial applications with the intent of operating at a high efficiency.

## 6.1 Future work

While filter types other than passive are briefly discussed in this work, they were not simulated. As such, any future work on this topic should include simulations of active filters & hybrid-active filters, allowing for numerical comparisons of filtering efficiency and practicality.

In the simulations performed for this work, mid-simulation changes in load demand and voltage were handled by changing the fire angle. In real-life applications, a tap-changing transformer may be used for voltage control. Although turn ratios for pre-built transformers can not be changed during a simulation in PLECS, future work should include a custom built tap-changer transformer model or a similar way of voltage control without changing firing angle.

Lastly, as passive components are ideal in PLECS, measuring filter losses is difficult. Including non-ideal components, or performing simulations using software that features realistic components, would allow for more accurate loss estimations.

# Bibliography


[1] Benoit Technologies, “Understanding Industrial Rectifiers: What Are They and How Do They Work?,” Benoit Technologies, Sep. 11, 2025. https://btlme.com/industrial-rectifiers/ (accessed May 25, 2026).

[2] “IEEE guide for the application and specification of harmonic filters,” IEEE Std 1531-2020 (Revision of IEEE Std 1531-2003), pp. 1–71, 2021, doi: https://doi.org/10.1109/IEEESTD.2021.9336377.

[3] “IEEE standard for harmonic control in electric power systems,” IEEE Std 519-2022 (Revision of IEEE Std 519-2014), pp. 1–31, 2022, doi: https://doi.org/10.1109/IEEESTD.2022.9848440.

[4] M. A. McGraw, A. Hoevenaars, J. Kotrla, and J. Greenwald, “Understanding the relationship between total harmonic distortion and total demand distortion in IEEE STD 519-2022: A practical discussion for compliance evaluations,” 2024, pp. 1–6. doi: https://doi.org/10.1109/PCIC47799.2024.10832187.

[5] A. Q. Al-Shetwi, M. A. Hannan, K. P. Jern, M. Mansur, and T.M.I. Mahlia, “Grid-connected renewable energy sources: Review of the recent integration requirements and control methods,” Journal of Cleaner Production, vol. 253, p. 119831, 2020, doi: https://doi.org/10.1016/j.jclepro.2019.119831.s

[6] E. Owen, “SCR is 50 years old [History],” Industry Applications Magazine, IEEE, vol. 13, pp. 6–10, Nov. 2007, doi: https://doi.org/10.1109/MIA.2007.907204.

[7] J. Hindmarsh and A. Renfrew, “Chapter 7 - Power-electronic/electrical machine drives,” Third Edition.Butterworth-Heinemann, 1996, pp. 232–294. doi: https://doi.org/10.1016/B978-075062724-5/50010-3.

[8] N. Mohan, W. P. Robbins, and T. M. Undeland, Power electronics : converters, applications, and design. Hoboken, Nj: Wiley, 2007.

[9] K. N. Mude, “8 - single-phase controlled rectifiers,” M. H. Rashid, Ed., Fourth Edition.Butterworth-Heinemann, 2018, pp. 209–231. doi: https://doi.org/10.1016/B978-0-12-811407-0.00008-8.

[10] [G. Rizk, S. Salameh, H. Y. Kanaan, and E. A. Rachid, “Design of passive power filters for a three-phase semi-controlled rectifier with typical loads,” 2014, pp. 590–595. doi: https://doi.org/10.1109/ICIEA.2014.6931233.

[11] Monolithic Power Systems, “Passive Filters for Harmonic Elimination,” Monolithicpower.com, 2024. https://www.monolithicpower.com/en/learning/mpscholar/power-electronics/power-quality-and-harmonics/passive-filters-for-harmonic-elimination

[12] PSCAD, "Passive Filter Design," Pscad.com, Jan. 19, 2003. https://www.pscad.com/webhelp/Master_Library_Models/Passive/Filters/Passive_Filter_De (accessed May 25, 2026).
[13] Y. Wang et al., "An optimized design method for doubletuned filters of AC filters Yard in converter station," in 2024 4th International Conference on Intelligent Power and Systems (ICIPS), pp. 253–258. doi: https://doi.org/10.1109/ICIPS64173.2024.10900053.
[14] X. Liu et al., "Optimized design method of Ctype damped filter for AC passive filters in converter station," in 2024 4th International Conference on Intelligent Power and Systems (ICIPS), pp. 197–205. doi: https://doi.org/10.1109/ICIPS64173.2024.10900111.
[15] Antonin Stampbach, "Active power filters for harmonics mitigation - imperix," imperix, Jun. 05, 2025. https://imperix.com/doc/implementation/active-power-filters-for-harmonics-mitigation?currentThread=active-power-filter
[16] D. Daftary and S. M. T, "Design and analysis of hybrid active power filter for current harmonics mitigation," 2019, pp. 1–4. doi: https://doi.org/10.1109/INDICON47234.2019.9029052.
[17] J. Phillips, "The Importance of the X/R Ratio in Short Circuit Calculations," Arc Flash Electrical Power Training | Brainfiller, Apr. 15, 2005. https://brainfiller.com/electrical-safety-codes-and-standards/x-r-ratio/ (accessed May 26, 2026).
[18] ABB, Transformer Handbook, 3rd ed. Zurich, Switzerland: ABB Power Technologies, 2010. [Online]. Available: electricalconnects.com [Accessed: May 25, 2026]
[19] K. Cheepati, S. Ali, and M. Surya. Kalavathi, "Overview of double tuned harmonic filters in improving power quality under non linear load conditions," International Journal of Grid and Distributed Computing, vol. 10, pp. 11–26, Jul. 2017, doi: https://doi.org/10.14257/ijgdc.2017.10.7.02.
[20] N. C. Brooks, F. Giardine, and Robert, "DC-Link capacitors for twice-line frequency power decoupling: Design-oriented figures-of-merit with empirical application," IEEE Transactions on Power Electronics, vol. 39, Art. no. 6, 2024, doi: https://doi.org/10.1109/TPEL.2023.3305153.
[21] J. A. Annankra and Y. Sefa-Boateng, "Evaluating the environmental impact of electronics production and the advancement in sustainable manufacturing processes," World Journal of Advanced Research and Reviews, vol. 28, no. 1, pp. 126–134, Oct. 2025, doi: https://doi.org/10.30574/wjarr.2025.28.1.3189.
[22] Carbonclick, "The environmental impact of electronics production and disposal," The environmental impact of electronics production and disposal, 2025. https://www.carbonclick.com/news-views/the-environmental-impact-of-electronics-production-and-disposal

# A

# Appendix 1: PLECS Simulation Files

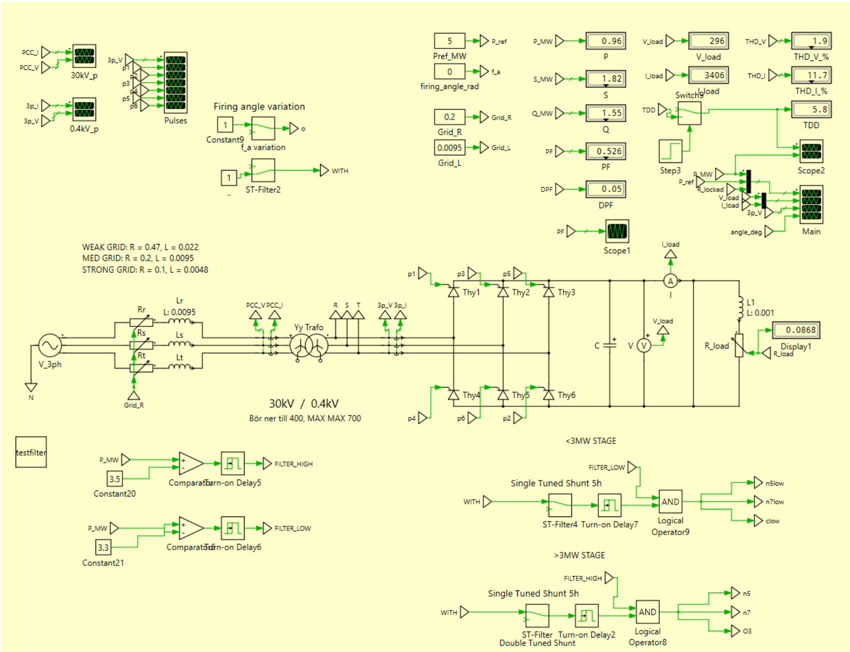


**Figure A.1:** 6-pulse rectifier with main displays and toggles.

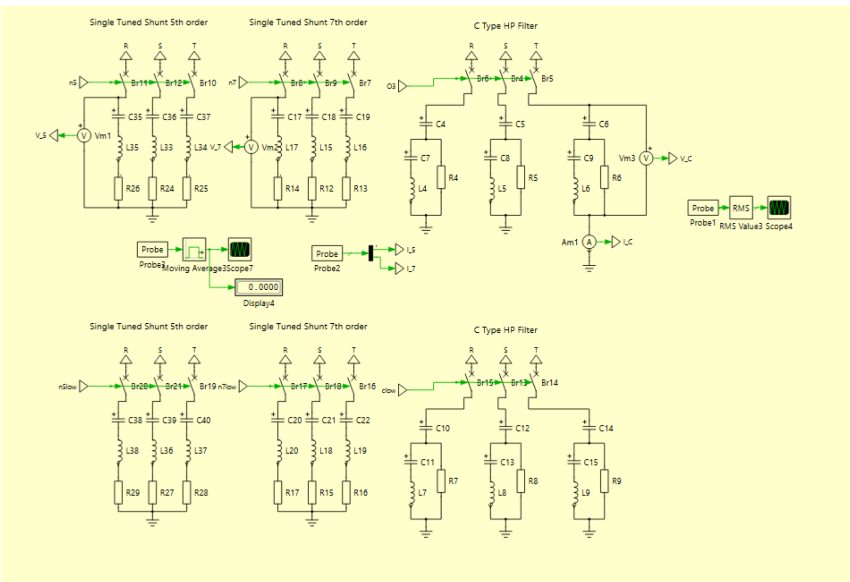


**Figure A.2:** 6-pulse rectifier filters.

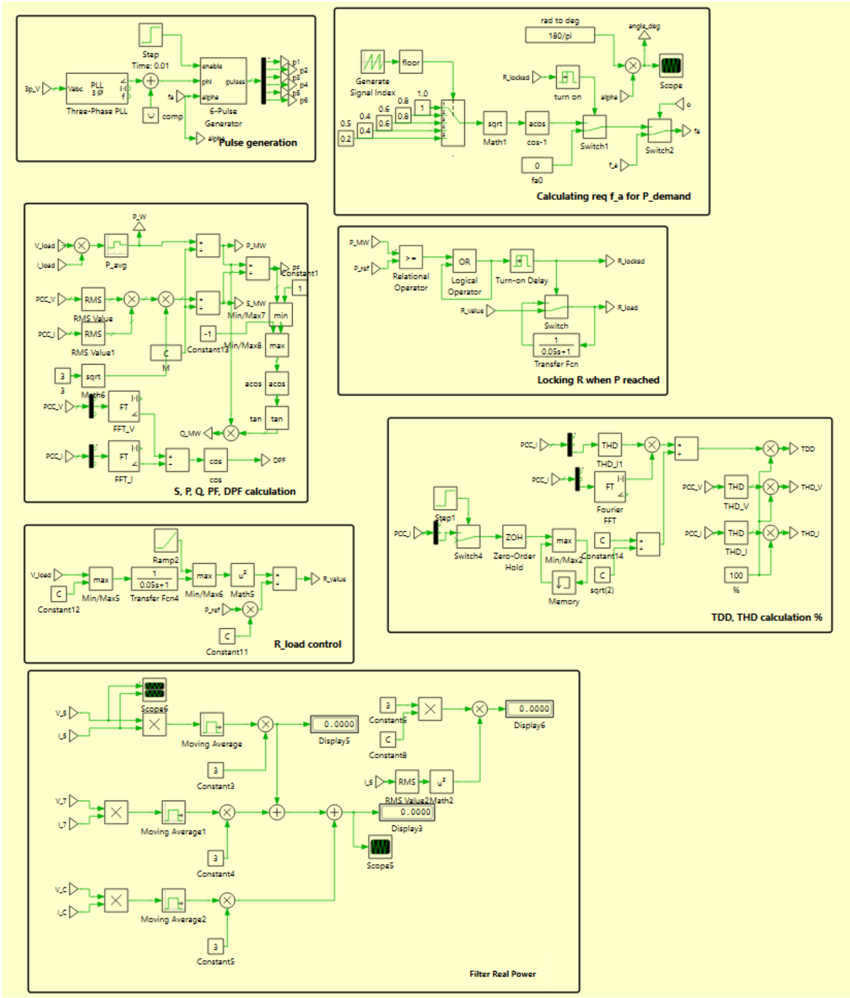


Figure A.3: 6-pulse rectifier calculation & logic blocks.

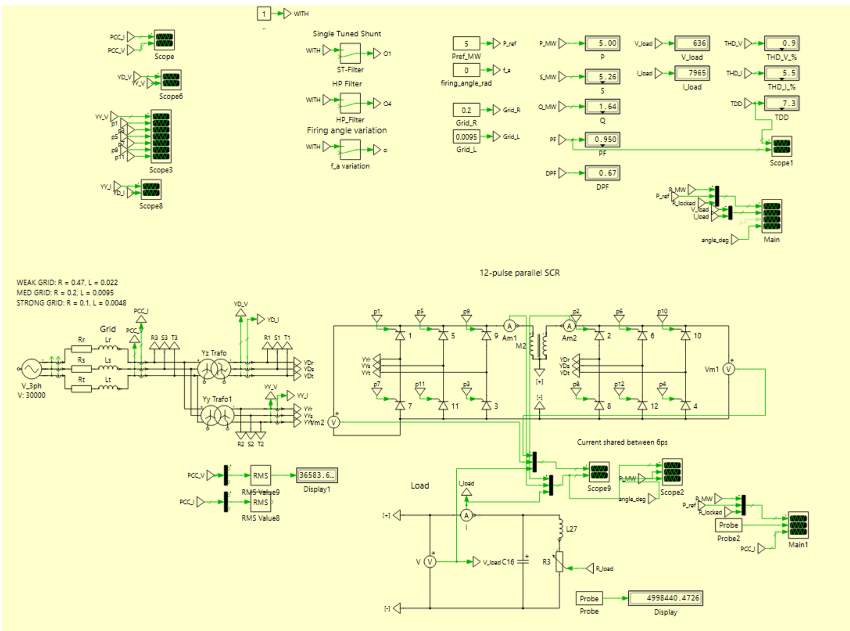


Figure A.4: 12-pulse rectifier with main displays and toggles.

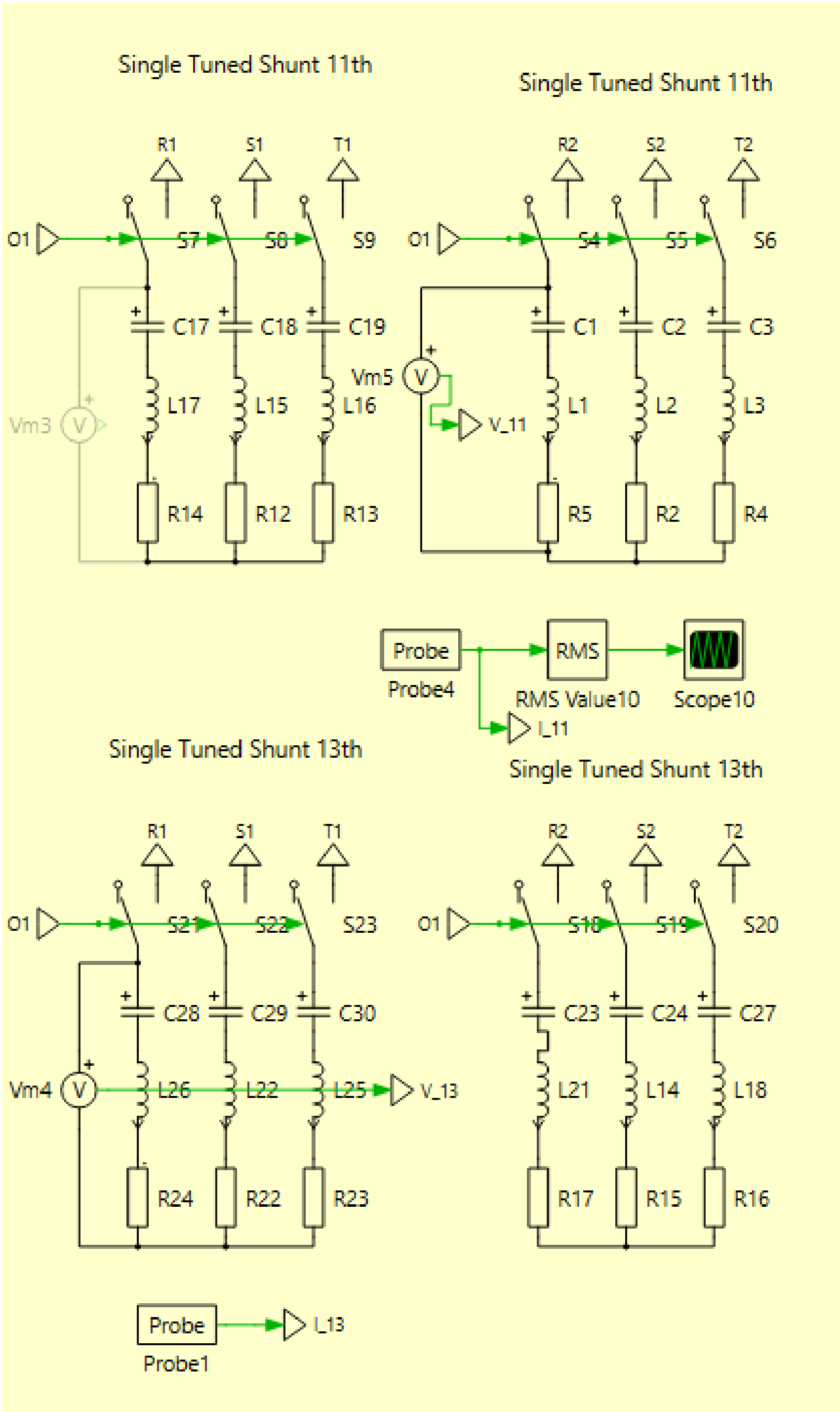


**Figure A.5:** 12-pulse rectifier filters.

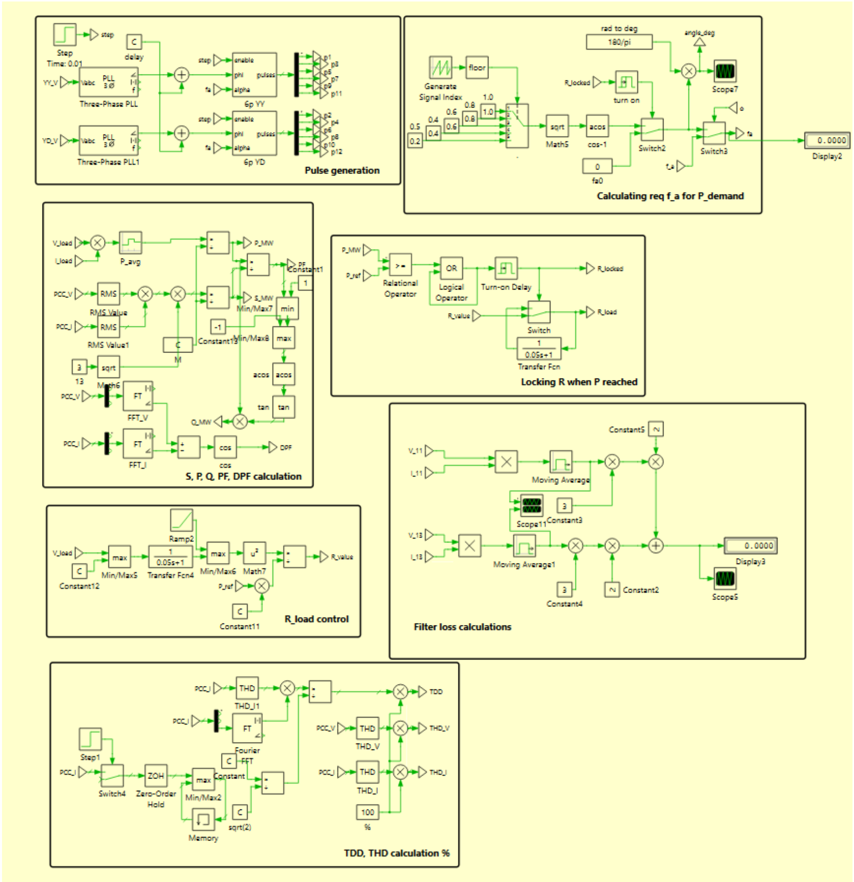


**Figure A.6:** 12-pulse rectifier calculation & logic blocks.

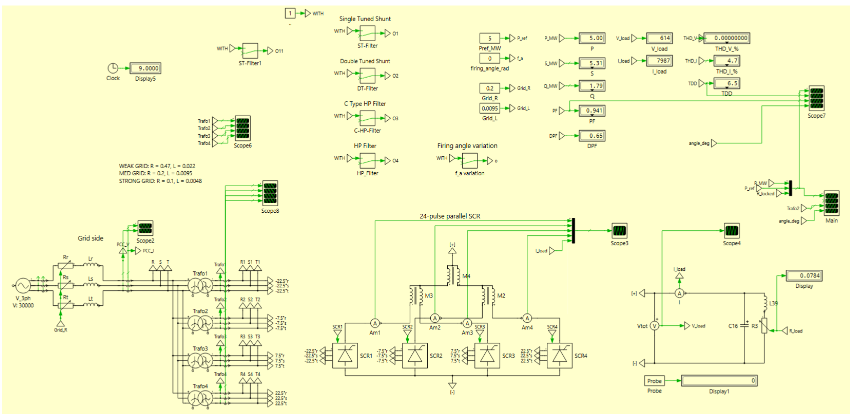


**Figure A.7:** 24-pulse rectifier with main displays and toggles.

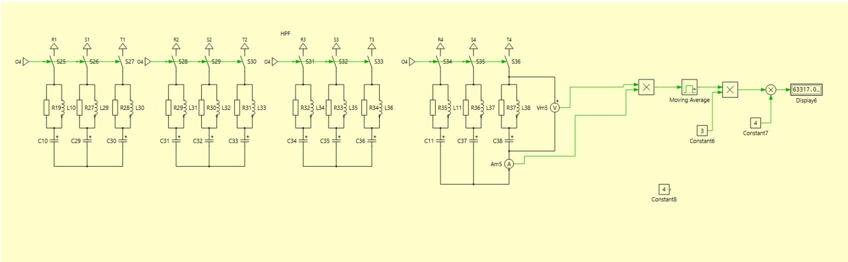

**Figure A.8:** 24-pulse rectifier filters.

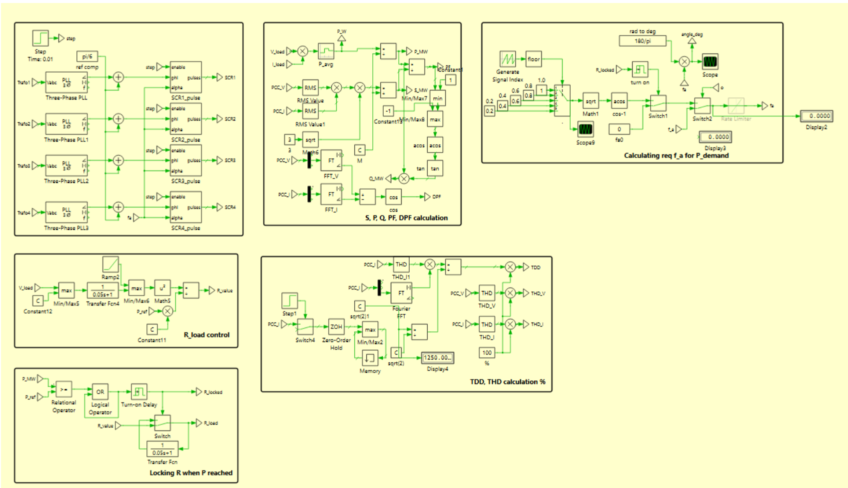

**Figure A.9:** 24-pulse rectifier calculation & logic blocks.

DEPARTMENT OF ELECTRICAL ENGINEERING
CHALMERS UNIVERSITY OF TECHNOLOGY
Gothenburg, Sweden
www.chalmers.se

CHALMERS
UNIVERSITY OF TECHNOLOGY